Response to Interactive Reviewer 1's comments on "Microphysics of Summer Clouds in Central West Antarctica Simulated by Polar WRF and AMPS" by Hines et al.

Response to summary.

Perhaps it is important here to emphasize our motivation. The AMPS forecasts are widely used in Antarctica and support operations – including aircraft flights – in this difficult and extreme environment (Bromwich et al. 2005; Powers et al. 2009, 2012, Wille et al. 2017). The weakness in representing clouds has been known for some time. A former member of the Polar Meteorology Group at The Ohio State University did a Master's Thesis that looked at the representation of clouds in AMPS (Pon 2015). Also, we have plenty of experience running Polar WRF in both hemispheres (e.g., Bromwich et al. 2013, 2018) and this includes looking at the representations of clouds by Polar WRF in the Arctic (Hines and Bromwich 2017). We are highly motivated to study how well AMPS is doing in representing Antarctic clouds and how such forecasts might be improved. The recent AWARE project (2015-2017) was an obvious opportunity enabling working with AMPS cloud issues.

We took care to avoid overarching statements about how one of the newer microphysics schemes was generally better than the others, since extensive testing would be required make such general statements. The observations at WAIS Divide during December 2015-January 2016 are not detailed enough to show comprehensive ice and liquid cloud microphysics. In particular there is little direct measurement of cloud ice beyond generic "cloud". More extensive measurements are available at McMurdo. That site, however, is strongly influence by the detailed topography of Ross Island, while WAIS Divide has greater regional representativeness. We prefer to start with WAIS Divide for this reason. Additional work will be done with the more detailed measurements at McMurdo, but we believe we should be familiar with the characteristics of WAIS Divide first.

The existing combination of cloud and microphysics observations at WAIS Divide, nevertheless, enable many comparisons of model to observations. Model biases in cloud water, for example, can be expected to be revealed. Our results do show more liquid simulated with some schemes, especially those that include elements of two-moment microphysics. The expected impact of liquid water on radiation is demonstrated in the simulation results.

We believe the comparison of the WSM5C microphysics schemes to the other schemes – which we refer to as more advanced schemes – is well founded. The WSM5C microphysics scheme is well-known in WRF modeling community to have difficulty simulating supercooled liquid water. More generally, representing supercooled liquid water is known to be difficult in numerical modeling studies. We have added the reference of Morrison and Pinto (2006) in this regard. Hugh Morrison's microphysics scheme, which was developed with the Arctic in mind is relatively successful in representing Arctic cloud water (Hines and Bromwich 2017 and references therein). This is known in the polar climate modeling community. So we believe the comparison of the

WSM5C scheme – a one-moment microphysics scheme which is a relatively older generation algorithm – to newer generation schemes is a reasonable thing to do.

AMPS is considering changing microphysics schemes for better cloud representation. Other schemes, however, are more computationally expensive (Jordan Powers, personal communication, 2018), so the cpu cost must be weighed versus the gain in results. Our research is relevant to this decision.

We added some scatter plots for a different method of model vs. observation analysis than shown in the original submission of the manuscript. The new figure is shown here. In Fig. 4a, the negative temperature bias in AMPS is shown to be larger when the observed temperature is above about -10ºC. Thus, AMPS is unlikely to well represent melting events. The error in longwave radiation shown in Fig. 4c is larger when the observed longwave radiation larger than about 200 W m^{-2}. That is AMPS is less accurate at times when clouds are likely to be present. In contrast, Morrison, Thompson and P3 better treat cases when the observed longwave radiation is relatively large. The AMPS error tends to be smaller with the longwave radiation is relatively small. That is, the error tends to be smaller when cloudiness is small.

It was a good suggestion to recommend the use of simulator for remote sensing observations, and we took this suggestion very seriously. So we obtained the CR-SIM cloud resolving model radar simulator 3.2 from Brookhaven National Laboratory. This includes software for representing MPL observations, and can produce cloud fraction output. We thought this would be ideal for comparisons with the cloud fractions based upon MPL. This simulator works with WRF output. It is designed for output from several WRF microphysics schemes. Unfortunately, the simulator results proved to be unworkable, and the MPL attenuation was not produced in the simulator output. As an alternative, we reduced the vertical span of our vertical plots of cloud fraction. This removes most of the height regions where the MPL observations were attenuation.

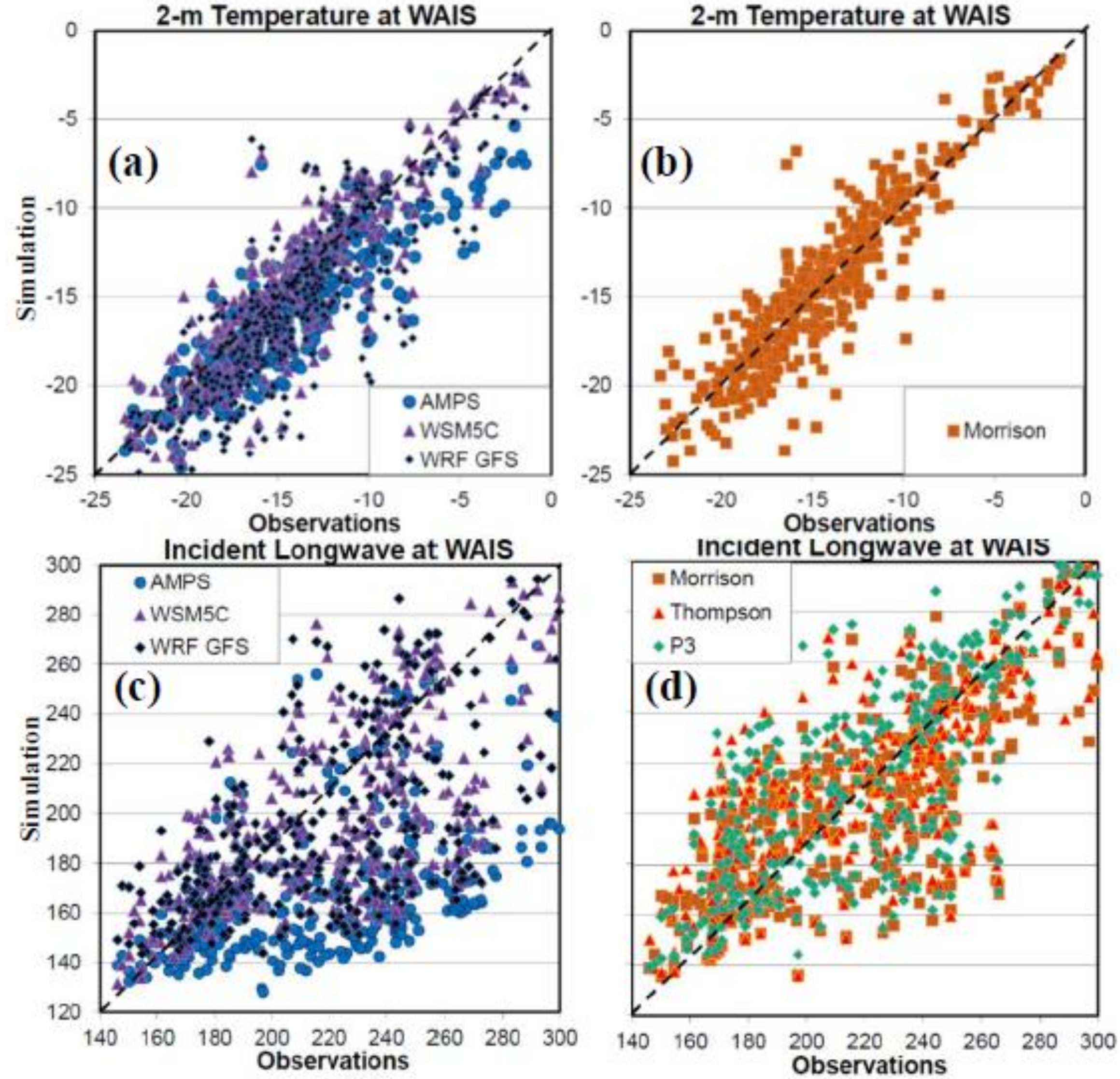

Figure 4: Scatter plots of observed values (horizontal axis) and simulated results (vertical axis) of 2 m temperature (°C) for (a) AMPS, WSM5C and WRF GFS and (b) Morrison, and downwelling longwave radiation (W m^{-2}) for (c) AMPS, WSM5C, and WRF GFS and (d) Morrison, Thompson and P3. The dashed line shows the 1 to 1 line.

Detailed Comments:

Page 2 line 19-28, P3 l5-6, P3 l10-11, P4 l3, P4 l11, P 5 l1, P5 l1-5, P 6 l4-5, P6 l22, P6 l25, P6 l28-29, P8 l26, P10 l11, P10 l13, P12 l14-15, P14 l19-20, P15 l1, P16 l11 and P17 129. The text has been modified to address these comments.

P3. l8. We have gone back and checked the Sibler et al. (2018) reference, and the modified text is consistent with the reference.

P4 l6-7. We were unable to connect this comment to any line in the first version of the manuscript.

P4 6-9. The text has been rearranged based upon this comment.

P4, l12-14. The AWARE site locations are added to Figure 1b and 2b.

P 4 l l29-31 and P14 l26. Thank you for proving the most recent community viewpoint on how the surface thermodynamic equation should be treated. First, we should provide some background on our use of the "surface energy balance" for Table 3 and Figure 7b. We had hoped to use the measurements of the conductive flux in the ice pack at WAIS Divide. Unfortunately, instrument errors resulted measurements of unacceptable quality. Previously, Nicolas et al. (2017) produced alternative estimates of the conductive flux by assuming a balance of terms, then solving for the "ground" term. This work was presented in the work published in refereed journal *Nature Communications*. The storage term could, of course, be large instantaneously, but should have a relatively small value when averaged over time compared to other terms in the thermodynamic equation. We think then this method provides a reasonable estimate of the conductive flux, given that quality direct measurements were unavailable. Again, these are previously published numbers.

P5 l9-12. To compensate for the attenuation of the lidar signal by hydrometers, we have added the lidar simulator from the CR-SIM Cloud Resolving Model (CRM) Radar Simulator version 3.2 to comparison between model-simulated hydrometers and remote sensing observations at WAIS Divide. This simulator is configured for WRF model output.

P5 l31. A reference is added for Tjernström et al. (2014).

P6 l1-2 and P6 l6-13. The text has been rearranged based upon these comments.

Page 6 l11. We added information on the levels. The lowest levels are at 10, 37, 73, and 119 m.

P6 l14. The smaller domains shown in Fig. 1a are nested domains. Thus, they are "forced" by the larger domains. We have modified the text slightly.

P6 l19. It was not possible to equalize all settings between AMPS and the Polar WRF 3.9.1 simulations. This was an important reason for the inclusion of the WSM5C simulation, since it would have the same microphysics scheme as AMPS, yet have the same settings, except for the microphysics scheme, as the Morrison, Thompson, and P3 simulations. Since we ultimately wished to compare our results to the observations at WAIS Divide, it was desirable to have a good framework for our comparison. We used the PBL scheme that we thought would give the best results. The addition of new simulation WRF GFS, discussed later, helps to bridge the gap between AMPS and WSM5C.

P6 l19-22. Large-scale data assimilation seeks to include many observations to set the analysis field. This may result in a smoothing of fields. Mesoscale data assimilation seeks to include mesoscale structures in the resulting field. So the goals of global data assimilation and mesoscale data assimilation are different. The risk/reward calculations are different. Mesoscale data assimilation tends to be more dependent on individual observations, as the goal is to represent fine features. An individual observation can influence both the global analysis field and the mesoscale data field derived in part from the global analysis field. In that sense the observation is "double dipping" but this is not an error. The key here is that data assimilation on different scales has different goals.

P6 l24-26. The AMPS source for sea ice fraction is now shown in the revised manuscript.

P8 l14. A reference is added for Cooper (1986).

P8 l18. Apparently, there is not a consensus as to the descriptions "Western Arctic" and "Eastern Arctic". We have changed the description of location of ASCOS in the revised manuscript.

P8 l30-31. The terminology "water friendly" and "ice friendly" is taken from the publication Thompson and Eidhammer (2014). We have had previous extensive discussions with Greg Thompson about this scheme. The wording has been changed in the revised manuscript.

P8 l8- P9 l6. We have added some words in section 3.2 on the differences between microphysics schemes.

P9 l14-21. The text has been rearranged based upon this comment.

P9 l21. We have checked and found no nudging is done in AMPS. There was some confusion in the preparation of the original manuscript because of a presentation by a former graduate student at Ohio State on the positive impact of "grid nudging" in WRF Antarctic forecasts that was inspired by AMPS forecasts. The manuscript has been changed to avoid confusion.

P9 l23-26. Please see the response to the summary explaining the importance of AMPS. We have added a simulation "WRF GFS" with the WSM5C microphysics and the GFS final analysis providing the initial and boundary conditions. We believe this helps to bridge the gap between the AMPS results, driven by the GFS forecast fields and the WSM5C simulation with Polar WRF 3.9.1 and driven by ERA-Interim.

P10 l5. It was not our intent to re-demonstrate in detail the West Antarctic warming discussed in the published paper Nicolas et al. (2017). The use of the word "demonstrated" in the original manuscript was unfortunate. The text has been changed.

We will take care in the submission of the final figures for quality and visibility. Unfortunately, the small size of figures in the first version limited visibility.

P10 l19-25. Yes, the difference between the simulations Morrison, Thompson and P3 is relatively small. No definitive claim can be made of superiority between these schemes. That could imply the fine detail differences between these more recent schemes has relatively small impact on the simulation results.

As to the WSM5C scheme, the addition of the new WRF GFS simulation helps. It has the same microphysics scheme as the WSM5C scheme, however it uses the GFS final analysis for initial and boundary conditions. This is not exactly the same as the GFS forecast used by AMPS (the final analysis is not available at forecast time, and AMPS is run prognostically). However, the GFS final analysis uses the same forecast system as the GFS forecasts. The simulations with the WSM5C scheme consistently produce too little cloud liquid, whether GFS or ERA-Interim is used for the initial and boundary conditions. Correspondingly, downwelling shortwave simulation is excessive and there is a deficit in downwelling longwave radiation. This is consistent with the experience of mesoscale modellers in the Arctic. The reference, Morrison and Pinto (2006), now used in the revised version, mentions that simulating supercooled liquid water is a known difficulty in the polar regions. Hugh Morrison's double-moment scheme has been known simulate supercooled water relatively well in multiple Arctic studies (several references are given in our earlier paper Hines and Bromwich 2017). In the present work, the three more recent microphysics schemes produce more liquid water, and have greater cloud forcing.

P11 1-6. The 2-m air temperature is close to the skin temperature, and the skin temperature is used for upwards longwave radiation at the surface and the calculation of conductive flux in the snowpack by the WRF Noah land surface model. So this temperature is important for the surface energy terms and the interaction therein. Therefore we choose to show the 2-m temperature in this paper. The 2-m temperature is also a widely-measured quantity, and at the height or near the height at which many other near-surface variables are measured.

Now, the surface boundary layer is of interest for the AWARE project, but our interest in this paper is the clouds and the related radiation. So we prefer not to divert attention away from the clouds and radiation by additional analysis of the boundary layer in this paper. We may look in greater detail at the boundary layer in our near-future AWARE work. This will probably involve the McMurdo observations that are more detailed than the WAIS divide observations.

The words have been changed about the description of biases in response to this comment. "Negative bias" and "positive bias" are now used in the text, and "cold bias" is less used in the revised manuscript.

P11 l19. The sentence is removed.

P11 l30-21. We change the explanation of how we determine the statistical significance.

P12 19-20 & l22-24. Perhaps it's understandable how discussion of the statistical significance of results for specific hours of the day versus that for all times could be confusing. We now mention in the text that Table 3 shows the biases for all times (rather than the bias for a specific time of day). It is easier to meet the criteria for statistical significance for all times, rather than for a specific time of day when the sample size is reduced.

P13 l29- P14 l14. We rearranged the discussion of the earlier satellite data studies in response to this comment.

P17 l3-4. Took this comment with high interest and sought to add CR-SIM Cloud Resolving Model (CRM) Radar Simulator version 3.2 to our comparison between model-simulated hydrometers and remote sensing observations at WAIS Divide. This simulator is configured for WRF model output.

P17 l21-22. We removed the sentence.

P17 l24-33. We removed some of the previous text. We added the sentence, "Similar to the profile displayed in Fig. 13a, the observations show a more shallow peak in the lower troposphere than in the simulations. (Fig. 14a)." The figure numbers in this reply are based upon the original submission of the manuscript.

Response to Interactive Reviewer 2's comments on "Microphysics of Summer Clouds in Central West Antarctica Simulated by Polar WRF and AMPS" by Hines et al.

Response to General Comments

Thank you for these comments. We have changed the wording describing the microphysics schemes. We might add though that we believe our previous words are not "promotional" as much as they are accurate descriptions of the current thought in the cloud modelling community. The one-moment WSM5C scheme represents an older approach to cloud modeling with a prognostic treatment of several hydrometers in terms of the mixing ratio, while the other schemes are from more recent generations of cloud modelling and include elements of two-moment microphysics schemes. Thus, the newer schemes predict both the mixing ratio and some measure of the cloud size distribution. Accordingly, they allow for a greater degree of freedom in the cloud hydrometers. We have had extensive discussions with Hugh Morrison and Greg Thompson on these microphysics schemes.

Here is some text we included from the discussion with Reviewer 1:

We believe the comparison of the WSM5C microphysics schemes to the other schemes – which we refer to as more advanced schemes – is well founded. The WSM5C microphysics scheme is well-known in WRF modeling community to have difficulty simulating supercooled liquid water. More generally, representing supercooled liquid water is known to be difficult in numerical modeling studies. We have added the reference of Morrison and Pinto (2006) in this regard. Hugh Morrison's microphysics scheme, which was developed with the Arctic in mind is relatively successful in representing Arctic cloud water (Hines and Bromwich 2017 and references therein). This is known in the polar climate modeling community. So we believe the comparison of the WSM5C scheme – a one-moment microphysics scheme which is a relatively older generation algorithm – to newer generation schemes is a reasonable thing to do.

AMPS is considering changing microphysics schemes for better cloud representation. Other schemes, however, are more computationally expensive (Jordan Powers, personal communication, 2018), so the cpu cost must be weighed versus the gain in results. Our research is relevant to this decision.

Since the role of the different boundary conditions and initial conditions has been discussed by both reviewers, we added analysis of a simulation with WSM5C microphysics scheme that has forcing by the GFS final analysis rather than ERA-Interim. The new simulation is called WRF GFS. The results of this simulation show a 2 m temperature cold bias (-1.5 °C) similar to that of AMPS (-1.6 °C). The longwave and shortwave radiation for WRF GFS have biases of the same sign and slightly larger magnitude than those of WSM5C simulation. For longwave, the bias for WSM5C is -14.8 W m^{-2} and -17.0 W m^{-2} for WRF GFS. The results of the new simulation supports the conclusion that the WSM5C microphysics has biases in the representation of clouds leading to too much downwelling shortwave and too little downwelling longwave radiation at the surface of West Antarctica.

We have done what we could to improve the figures. We recognize that the reduction in size to the manuscript specifications in the initial submission reduces the visibility of figures. We have attached selected larger figures to this response. We will see to it that high quality figures are sent to the journal for final publication.

Observations of clouds by surface observers or by remote sensing techniques differentiate between "cloud fraction" and "cloud frequency". For comparison to the model, the distinction is not so important since model cloud fraction tends to be zero or one (either by the vertically-integrated hydrometer method taken from Fogt and Bromwich [2008] or by a local threshold value set at a hydrometer mixing ratio of 10^{-6}). We have sought to make the manuscript more clear on this point.

Specific Comments:

Page 2, Line 8, Page 3, Line 29, Page 4, Line 10, Page 5 Line 13, Page 7 Line 18, Page 8 Line 18, Page 11 Line 4, Page 11 Line 30-35, Page 12 Line 14 and Page 12 Line 26. The text has been modified to address these comments.

Page 3, Line 30, Page 15, Line 6 and Page 19, Line 5-11. The text has been rearranged based upon these comments.

Page 4, Line 12. The field site locations are added to Figures 1b and 2b.

Page 13, Line 12. The new simulation WRF GFS helps here in that it shows the radiation biases do not greatly change between forcing by GFS or ERA-Interim. The results are consistent with simulations with the WSM5C scheme showing too little liquid water, too little downwelling longwave radiation and too much downwelling shortwave radiation. This scheme is rather well known among WRF users in the polar regions for simulating too little liquid water. We have added the reference to Morrison and Pinto (2006) about the known difficulty of models simulating liquid water in polar regions. Our simulations with the more recent microphysics schemes produce more liquid water and greater cloud radiative effect.

Page 16, Line 4. The observations that could be taken at WAIS Divide during December 2015 and January 2016 were limited, due to the remoteness of the location. The main observational location for AWARE was at the McMurdo station that is a major freight transit point in Antarctica. We must use what observations are available for WAIS. Fortunately, lidar observations were available at WAIS, and the observations can be processed into cloud fraction following Sibler et al. (2018). We are making use of the available observations for comparisons to the modeling results.

Page 16, Line 16. Observations of clouds by surface observers or by remote sensing techniques differentiate between “cloud fraction” and “cloud frequency”. For comparison to the model, the distinction is not so important since model cloud fraction tends to be zero or one (either by the vertically-integrated hydrometer method taken from Fogt and Bromwich [2008] or by a local threshold value set at a hydrometer mixing ratio of 10^{-6}). We have sought to make the manuscript more clear on this point.

Table 1. We have added the driving source of the meteorological fields to Table 1. We believe the detailed description of the microphysics schemes is best shown in Section 3.2.

Figures 8-12. Unfortunately, the similarity of the time series makes it difficult to differentiate some of the lines. Larger size versions of Figures 8-10 (old ordering according to the previous submission) are attached here for better clarity. Figures 11 and 12 have been replaced due to the introduction of the lidar simulator.

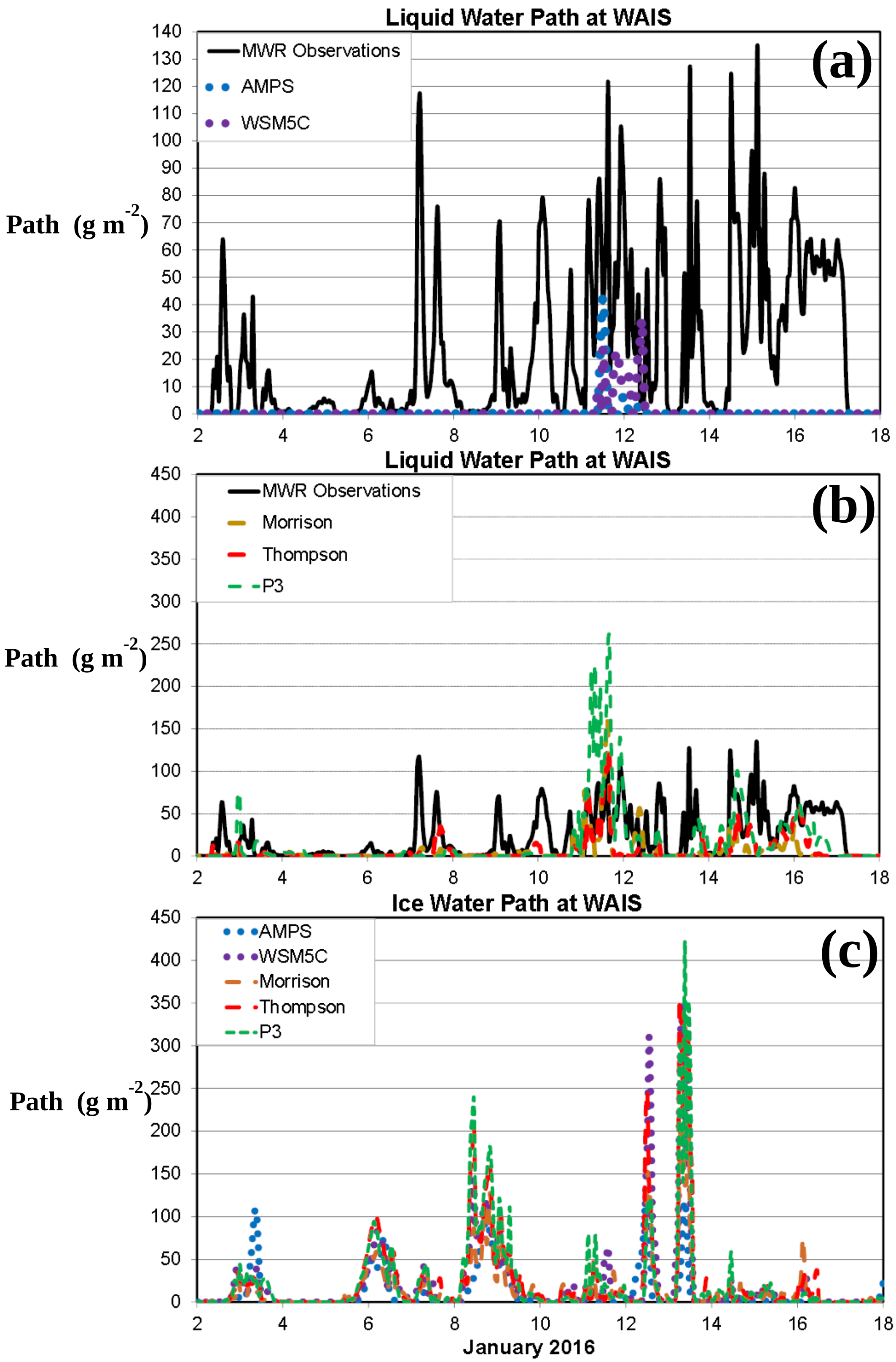

Figure 8: Time series of (a) and (b) liquid water path (mm) and (c) ice water path (mm) over 0000 UTC 2 January–0000 UTC 18 January 2016. Microwave radiometer (MWR) observations are available for liquid water path and are shown by solid curves in (a) and (b). Values for AMPS and the WSM5C simulation are shown in (a) and (c), while values for the three simulations with advanced microphysics schemes are shown in (b) and (c).

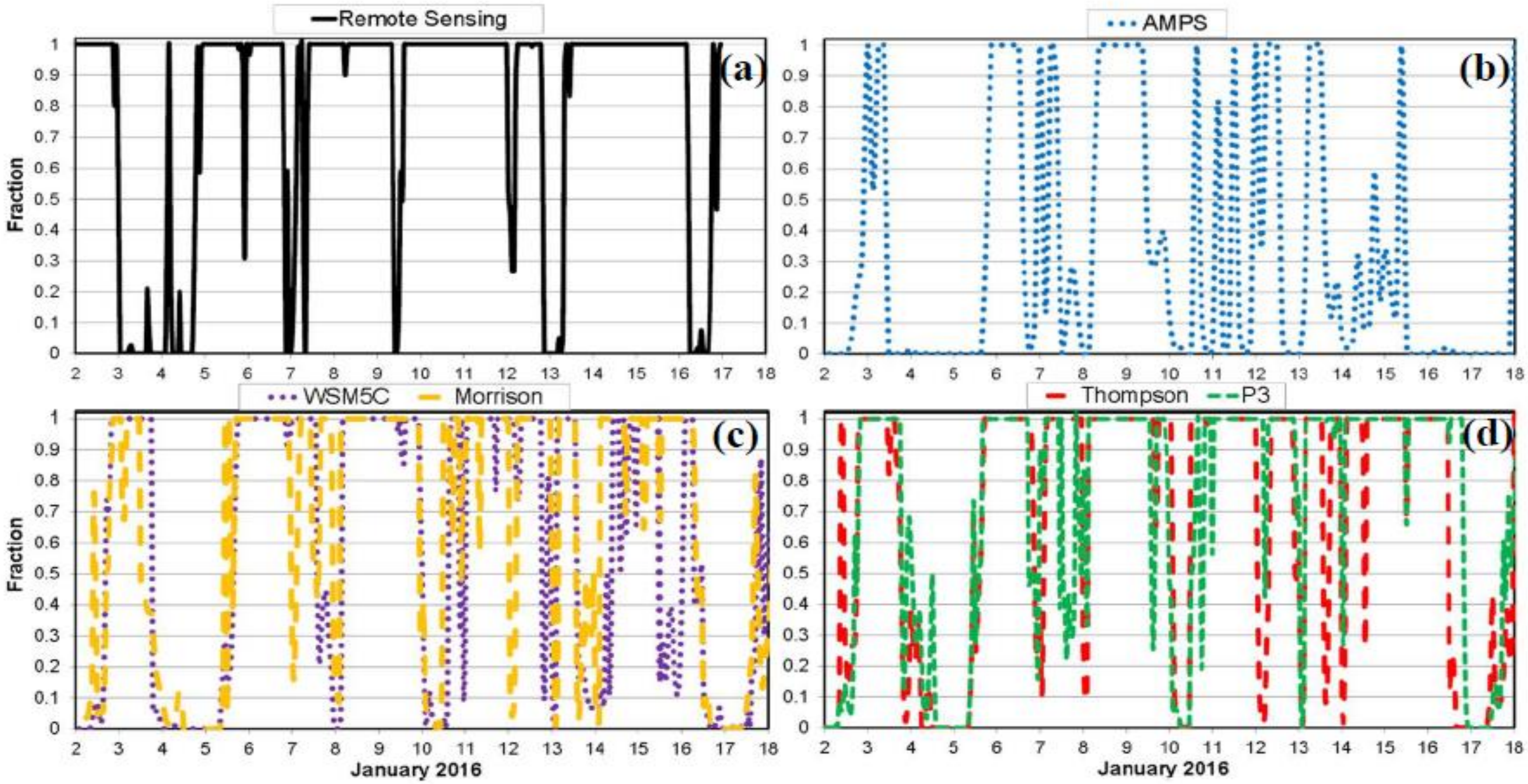

Figure 9: Time series of cloud fraction for (a) remote sensing observations, (b) AMPS, (c) the WSM5C and Morrison simulations, and (d) the Thompson and P3 simulations. Model values of cloud fraction are based upon the Fogt and Bromwich (2008) algorithm using liquid water path and ice water path.

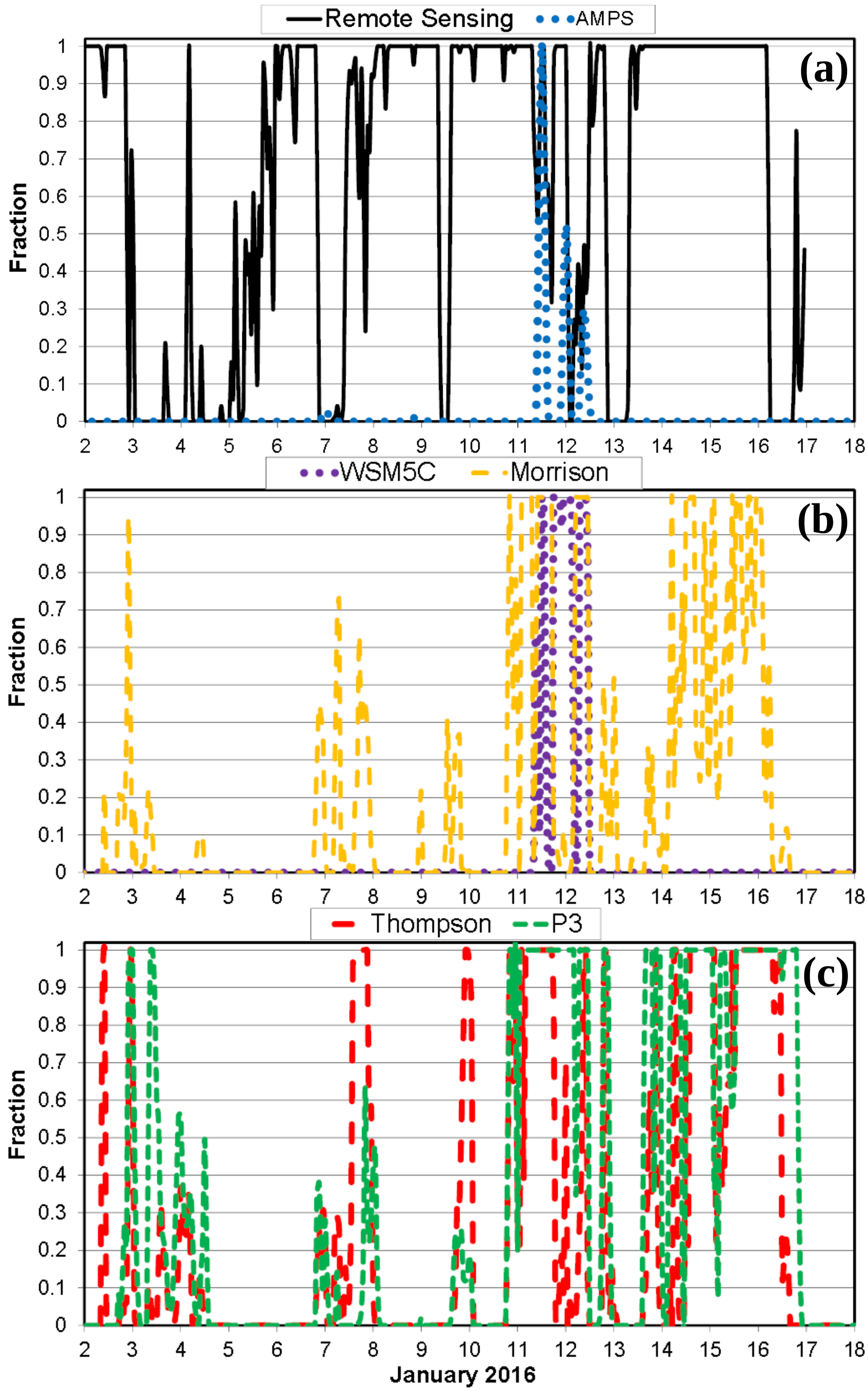

Figure 10: Time series of liquid cloud fraction for (a) remote sensing observations and AMPS, (b) the WSM5C and Morrison simulations, and (c) the Thompson and P3 simulations. Model values of cloud fraction are based upon the Fogt and Bromwich (2008) algorithm.

Microphysics of Summer Clouds in Central West Antarctica Simulated by Polar WRF and AMPS

Keith M. Hines[1], David H. Bromwich[1,2], Sheng-Hung Wang[1], Israel Silber[3], Johannes Verlinde[3], Dan Lubin[4]

[1]Polar Meteorology Group, Byrd Polar & Climate Research Center, The Ohio State University, Columbus, OH, 43210, USA

[2]Atmospheric Sciences Program, Department of Geography, The Ohio State University, Columbus, OH, 43210, USA

[3]Department of Meteorology and Atmospheric Sciences, The Pennsylvania State University, University Park, PA, 16802, USA

[4]Scripps Institution of Oceanography, University of California, San Diego, La Jolla, CA, 96802, USA

Submitted to Atmospheric Chemistry and Physics

November 2018

Revised June 2019

Formatted: Font color: Text 1

Formatted: Font color: Text 1

Correspondence to: Keith M. Hines (hines@polarmet1.mps.ohio-state.edu)

Abstract. The Atmospheric Radiation Measurement (ARM) West Antarctic Radiation Experiment (AWARE) provided a highly detailed set of remote sensing and surface observations to study Antarctic clouds and surface energy balance, which have received much less attention than for the Arctic due to greater logistical challenges. Limited prior Antarctic cloud observations has slowed the progress of numerical weather prediction in this region. The AWARE observations from WAIS Divide during December 2015 and January 2016 are used to evaluate the operational forecasts of the Antarctic Mesoscale Prediction System (AMPS) and new simulations with Polar WRF 3.9.1. The Polar WRF 3.9.1 simulations are conducted with the WRF single-moment 5-class microphysics (WSM5C) used by AMPS and with newer generation microphysics schemes. advanced microphysics schemes and with the WRF single-moment 5-class microphysics (WSM5C) also used by AMPS. AMPS simulates few liquid clouds during summer at WAIS Divide, inconsistent with observations of frequent low-level liquid clouds. Polar WRF 3.9.1 simulations show that this result is a consequence of WSM5C. More advanced microphysics schemes simulate more cloud liquid water and produce stronger cloud radiative forcing, resulting in downward longwave and shortwave radiation at the surface more in agreement with observations. Similarly, increased cloud fraction is simulated with the more advanced microphysics schemes. All of the simulations, however, produce smaller net cloud fractions than observed. Ice water paths vary less between the simulations than liquid water paths. The colder and drier atmosphere driven by GFS initial and boundary conditions for AMPS forecasts produces lesser cloud amounts than the Polar WRF 3.9.1 simulations driven by ERA-Interim.

Formatted: Font color: Auto

1 Introduction

West Antarctica is among the most rapidly warming locations on Earth, and its warming is closely linked with global sea level rise (Rignot, 2008: Turner et al., 2006; Steig et al., 2009; Bromwich et al., 2013a, 2014). Recent paleoclimate work links temperature increases of a few degrees with past sea level increases of several meters due to disintegration of parts of the Antarctic Ice Sheet (DeConto and Pollard, 2016). Additional rise in Antarctic summer temperatures could lead to more frequent and extensive surface melting of the West Antarctic Ice Sheet (WAIS) (e.g., Nicolas and Bromwich, 2014). Conversely, increased temperatures can result in greater evaporation over the oceans and increased snowfall over Antarctica (Nicolas and Bromwich, 2014). The observational evidence shows West Antarctic warming since the 1950s (Bromwich et al., 2013a). Yet, there is disagreement about the cause, magnitude, seasonality and spatial extent of this warming due to regional and temporal gaps in the observational record and the overlapping influences of the El Niño-Southern Oscillation, the Southern Annular Mode, greenhouse gases, and ozone (e.g., Fogt et al., 2011; Bromwich et al., 2013a; Clem and Fogt, 2013; Hosking et al., 2016; Nicolas et al., 2017; Screen and Simmonds, 2012).

Unlike the elevated ice mass of East Antarctica, West Antarctica is highly prone to intrusions of moist air from the Southern Ocean (Nicolas and Bromwich, 2011, Scott et al., 2017). Thus, the West Antarctic climate is much more ocean-dominated than that of the colder and drier East Antarctica.

Moisture flux over West Antarctica leads to cloud formation. Clouds alter the net surface radiative flux and can thus impact the onset, extent, intensity, and duration of surface melting, refreezing, and ultimately meltwater control on cryospheric dynamics or runoff into the ocean (van Trincht et al., 2016). Modelling studies have shown that changes in cloud properties over Antarctica may impact regions of the globe well beyond high southern latitudes (Lubin et al., 1998). Moreover, Antarctic clouds have different characteristics than Arctic clouds (Hogan 1986; Bromwich et al., 2012; Grosvenor et al., 2012; O'Shea et al., 2017). Antarctica can have very low ice nuclei (IN) concentrations (Hogan, 1986; Grosvenor et al., 2012; O'Shea et al., 2017). Silber et al. (2018a) show that cloud thickness at McMurdo Station peaks in austral winter, possibly due to cyclone activity, while Arctic cloud thickness peaks in boreal summer (Shupe, 2011). O'Shea et al. (2017) note significantly different types and concentrations of cloud condensation nuclei (CCN) and ice nuclei (IN) are expected between the Arctic and Antarctic due to the minimal anthropogenic sources at high southern latitudes. Aerosols tend to peak in winter and spring in the Arctic with a minimum during summer, while Antarctic aerosols tend to peak in austral summer and fall and are reduced during winter (e.g., Wagenbach et al., 1988; Schmeisser et al., 2018). Consequently, it's uncertain how well the findings of the various Arctic field programs and modelling experiments translate to Antarctica.

Formatted: Font color: Auto

Formatted: Font color: Auto

Formatted: Font color: Auto

Clouds, including liquid water clouds, have a strong modulation on the local climate (Nicolas and Bromwich, 2011; Bromwich et al., 2012; Scott et al., 2017; Silber et al., 2018a). A supercooled liquid cloud is likely to be more optically thick than a fully glaciated ice cloud (Shupe and Intrieri, 2004; Grosvenor et al., 2012; McCoy et al., 2015). Arctic cloud modelling studies find that cloud liquid water is frequently underrepresented in simulations with bulk microphysics schemes, and this can result in too little longwave radiation and too much shortwave radiation reaching the surface (e.g., Morrison and Pinto, 2006).

Formatted: Font color: Auto

Unfortunately, there have been few Antarctic field programs to detail cloud microphysical properties (e.g., Bromwich et al., 2012; Lachlan-Cope et al., 2016; Scott and Lubin, 2016). One study in the past decade by the British Antarctic Survey examined clouds over the Antarctic Peninsula (e.g., Grosvenor et al., 2012; Lachlan-Cope et al., 2016). Lachlan-Cope et al. (2016) found large differences in ice crystal concentrations between the clouds on the eastern and western sides of the peninsula, while Grosvenor et al. (2012) found elevated ice crystal concentrations with relatively warm temperature between -0.4 and -6.6°C. They also found that several widely used IN parameterizations poorly represented the observed relationship between ice particle concentration and temperature. Accordingly, clouds are frequently poorly represented in numerical simulations for Antarctica (e.g., Bromwich et al., 2013b; King et al., 2015). The following sections discuss efforts to evaluate and improve the simulation of Antarctic clouds. The recent AWARE project is discussed in Sect. 2, while Sect. 3

describes the Polar WRF simulations for this project, including AMPS numerical weather prediction forecasts for Antarctica. Results are discussed in Sect. 4, and Conclusions are given in Sect. 5.

The prime motivation for this work, as noted by Witze et al. (2016), is that there has been little in-place atmospheric science or climatological field work over interior West Antarctica since 1967, when a weather balloon program ended. A few automatic weather stations there provide direct meteorological information since 1980 (Lazzara et al., 2012). There is a need to quantify the impact of continental and oceanic air masses on the local hydrology and surface energy balance. Furthermore, there is a need for observations that can enable improved numerical simulations, both regional and global, through better representation of Antarctic clouds. The scarcity of cloud observations and well-tested simulations has so far inhibited significant progress. The work presented here may contribute to improvements to the AMPS simulations of clouds being sought by NCAR if computational efficiency can be achieved (Jordan Powers, personal communication 2018). Furthermore, we seek to evaluate and improve the numerical weather prediction for Antarctica, where the sparse observational network, the physics of the polar atmosphere, and the steep terrain challenge model capabilities (Bromwich et al., 2012). The need for accurate weather forecasting to support logistical and scientific activities has been important since the earliest Antarctic explorations

Formatted: Font color: Auto

Formatted: Font color: Auto

Formatted: Font color: Auto

Formatted: Font color: Auto

Formatted: Font color: Auto

2 AWARE

The Atmospheric Radiation Measurement (ARM) West Antarctic Radiation Experiment (AWARE, Witze et al. 2016) is a recent robust field program to study clouds and their impacts on atmospheric radiative transfer over the Antarctic continent. The prime motivation for AWARE was that there have been no substantial atmospheric science or climatological field work on WAIS in decades using suites of advanced equipment (Witze et al., 2016) other than a few automatic weather stations that provided direct meteorological information since 1980 (Lazzara et al., 2012).

AWARE used the joint capabilities of the U.S. Antarctic Program, managed by the National Science Foundation, and the Department of Energy's second ARM Mobile Facility (AMF2) to provide quantitative data about energy components, changing air masses, and cloud microphysical data to improve model simulations of the ice sheet as influenced by earth system processes.. The AMF2 consists of a collection of lidars, radars, and radiometers taking remote-sensing observations of the Antarctic clouds combined with in situ instruments documenting the atmospheric state, but more comprehensive observations are needed.. There is a need to quantify the impact of continental and oceanic air masses on the local hydrology and surface energy balance. Furthermore, there is a need for observations that can enable improved numerical simulations, both regional and global, through better representation of Antarctic clouds. The scarcity of cloud observations and well-tested simulations has so far inhibited significant progress.

Beginning late November 2015, AMF2 was deployed to Antarctica to make the first well-calibrated climatologicalmost extensive suite of measurements in more than 40 years (Witze et al., 2016). The primary AWARE site was McMurdo Station (77.85°S, 166.72°E) at the southern tip of Antarctica's Ross Island where observations took place between November 2015 and January 2017. A smaller suite of instruments was also deployed to WAIS Divide (79.468°S, 112.086°W, 1803 m above sea level) for 4756 days during the early and middle parts of austral summer (DecNovember 2015 - January 2016).

The WAIS Divide component of the AWARE field campaign ran from 4 December 2015 through 18 January 2016. A suite of ARM Mobile Facility instruments (Mather and Voyles, 2013) optimized for surface energy budget observations was moved from McMurdo to the WAIS Divide site during this period. Estimates of upper-air temperature and moisture were obtained from six-hourly rawinsonde launches and continuous retrievals from a profiling microwave radiometer (MWR, Morris 2006). Liquid water path (LWP) was extracted from a co-location of the MWR with a G-Band Vapor Radiometer Profiler (Cadeddu, 2010). The uncertainty of observed LWP is 10 g m^{-2} (Cadeddu et al., 2009).

Upwelling shortwave and longwave radiative flux components were measured by a Surface Energy Balance system (SEBS, Cook, 2018). Downwelling flux components were measured by a Sky Radiation System, which consists of a normal incidence pyrheliometer, shaded pyranometers and pyrgeometers (Dooraghi et al., 1996). The global downwelling shortwave flux was computed as in Nicolas et al. (2017). Surface fluxes for sensible and latent heat are derived according to the algorithm of Andreas et al. (2010). Near-surface measurements of temperature, moisture and wind speed were measured by the ARM surface meteorological instrumentation (Holdridge and Kyrouac, 1993). Instruments at WAIS were unable to obtain reliable measurements of the heat flux within the ice pack. As an alternative, estimates of the conductive heat flux from the ice surface and the underlying ice were taken from Nicolas et al. (2017) who calculated the residual of other terms in the surface energy balance.Furthermore, estimates of the conductive heat flux from the ice surface and the underlying ice were taken from Nicolas et al. (2017) who calculated the residual of other terms in the surface energy balance.

A cloud mask (derived from detected hydrometeor-bearing air-volumes) is used to determine the cloud and liquid occurrence fractions at WAIS Divide associated with the method of Silber et al. (2018a). In brief, depolarization micropulse lidar (MPL; Flynn et al., 2007) observations which were processed at Penn State (Silber et al., 2018b) are used to generate a linear depolarization ratio (LDR) versus log-scaled particulate backscatter cross-section two-dimensional histogram. This histogram, which is based on the full MPL data set from the WAIS Divide (after rough estimation of the particulate backscatter cross-section; see that can identify the hydrometer categories (Silber et al., 2018b,c)), is utilized for the determination of the hydrometeor population boundaries within the LDR-backscatter parameter space, followed by the classification of the lidar returns.

Formatted: Font color: Auto

Formatted: Font color: Auto

Hourly time series of total hydrometeor and liquid-cloud fractions were calculated from the processed cloud and liquid masks (with column integration). The occurrence fractions were normalized relative to the hourly MPL data availability, under the assumption that the measured period provided an acceptable representation of the whole hour. It should be noted that the MPL pulse can occasionally be completely attenuated by optically thick cloud layers (for example, as part of a frontal system). Therefore, the real cloud top, geometrical cloud thickness, and potentially, the liquid occurrence are underestimated by the MPL in these situations.

3 Polar WRF simulations

The advanced research Weather Research and Forecasting model (WRF) is an extensively used community numerical weather prediction model for numerous applications world-wide (e.g., Skamarock et al., 2008). Most of the polar optimizations for Polar WRF are added in the Noah LSM (Barlage et al., 2010) and improve the representation of heat transfer through snow and ice (Hines and Bromwich, 2008; Hines et al., 2015). Fractional sea ice was implemented in Polar WRF by Bromwich et al. (2009), followed by the addition of specified variable sea ice thickness, snow depth on sea ice, and sea ice albedo. These updated options were developed by the Polar Meteorology Group (PMG) at Ohio State University's Byrd Polar and Climate Research Center and were included in the standard release of WRF (https://www.mmm.ucar.edu/weather-research-and-forecasting-model) with the help of the Mesoscale and Microscale Meteorology Division at NCAR (Hines et al., 2015). Hines et al. (2011) made comparisons for cloud and radiation quantities between Polar WRF 3.0.1.1 simulations and observations at the North Slope of Alaska ARM site.

Formatted: Font color: Auto

Recently, Deb et al. (2016) evaluated Polar WRF 3.5.1 versus near-surface observations from West Antarctica. They found that pressure is simulated with high skill, and wind speed is generally well represented. The timing and amplitude of strong wind events were well captured. There were weaknesses in the diurnal cycle of temperature, especially denoted by a cold summertime minimum temperature bias. This was attributed to a negative bias in downwelling longwave radiation, consistent with clouds over Antarctica being poorly represented by models (e.g., Bromwich et al., 2012, 2013b; King et al., 2015; Listowski and Lachlan-Cope, 2017). Arctic modelling studies, however, suggest reason for optimism as Hines and Bromwich (2017) improved the representation of low-level liquid clouds by Polar WRF 3.7.1 with adjustments to the microphysics for simulations of the Arctic Summer Cloud-Ocean Study (ASCOS, Tjernström et al. 2014) near the North Pole during August-September 2008.

Formatted: Font color: Auto

3.1 AMPS

~~A goal for the AWARE project is to evaluate and improve the numerical weather prediction for Antarctica, where the sparse observational network, the physics of the polar atmosphere, and the steep terrain challenge model capabilities (Bromwich et al., 2012). The critical need for accurate weather forecasting to support logistical and scientific activities has been acute since the earliest Antarctic explorations.~~ To improve forecasting support for the U.S. Antarctic Program, the National Science

Foundation's Office of Polar Program initiated the Antarctic Mesoscale Prediction System (AMPS, Powers et al., 2012) in 2000. AMPS is a real-time numerical weather prediction with Polar WRF through a collaboration between the National Center for Atmospheric Research (NCAR) and the PMG. AMPS supports a variety of scientific and logistical needs for its international user base and has reduced costly flight turn-arounds between Christchurch, New Zealand and the McMurdo station (Powers et al., 2012).

For the time of the AWARE WAIS case study, the AMPS grid system consists of a series of nested domains with 60 vertical levels between the surface and the model top at 10 hPa. There are 12 layers in the lowest 1 km, with the levels nearest the surface at 10, 37, 73, and 119 m. ~~The lowest level is approximately 8 m above the surface, and 12 layers are in the lowest 1 km.~~ The outermost domain had 30 km horizontal resolution and covered Antarctica and much of the Southern Ocean (Fig 1a). Grid 2 had 10 km resolution and covered the Antarctic continent. Four additional higher resolution nested domains (3.3 km or 1.1 km) covered the Antarctic Peninsula, the South Pole and the region near McMurdo. For the present study, Grid 2 fields ~~only Grid 2 fields~~from the AMPS forecasts are used, and results are bilinearly interpolated to WAIS Divide from the four nearest grid points. Lateral boundary conditions for the outer AMPS domain and initial conditions, including sea ice fraction, are provided by ~~the Global Forecast System~~National Snow and Ice Data Center ~~(GFS, NOAA Environmental Modeling Center, 2003), a global forecast system run by the U.S. National Centers for Environmental Prediction, and were updated every 6 hr~~. The mesoscale representation in the initial fields is~~are~~ enhanced by the assimilation with 3-D variational data assimilation (Barker et al., 2004). Ingested fields include surface data, upper-air soundings, aircraft observations, geostationary and polar-orbiting satellite atmospheric motion vectors (AMVs), Constellation Observing System for Meteorology, Ionosphere, and Climate (COSMIC) GPS radio occultations, and Advanced Microwave Sounding Unit (AMSU) radiances. Twice daily~~Two~~ AMPS forecasts are begun ~~each day starting~~ from analyses at 000 UTC and 1200 UTC of the Global Forecast System (GFS, NOAA Environmental Modeling Center, 2003), a~~GFS~~ global forecast system run by the U.S. National Centers for Environmental Prediction~~analyses at 0000 UTC and 1200 UTC~~. For the current study we use AMPS output for forecast hours 12 - 21 at 3 hr intervals. Thus, our AMPS fields have a spin-up of a minimum of 12 hrs, with the possibility of ~~fluctuations~~jumps every 12 hrs due to the change toward a more recent~~in~~ initialization time. AMPS forecast fields in original WRF format are available from http://www.earthsystemgrid.org/project/amps.html. Selected AMPS output fields for March 2006 - December 2016 for Grids 2-6 can be downloaded from http://polarmet.osu.edu/AMPS/.

The scarcity of Antarctic meteorological observing stations and satellite blackout periods that can coincide with peak aircraft flight times increase the need for AMPS accuracy. Wille et al. (2017) note that unpredicted fog, low ceilings, and high winds lead to costly flight mission failures over Antarctica, thus accurately predicting acceptable flight windows is essential to prevent ~~costly~~ delays for science missions and cargo transportation. Unfortunately, AMPS has been shown to underestimate low clouds over the Antarctica (Wille et al., 2017). According to Pon (2015) the cloud fraction product in AMPS is so

Formatted: Font color: Auto

Formatted: Font color: Auto

Formatted: Font color: Auto

Formatted: Font color: Auto

Formatted: Font color: Auto

Formatted: Font color: Auto

Formatted: Font color: Auto

unreliable that most forecasters rely more on AMPS relative humidity as a proxy for cloud predictions. Therefore, addressing the cloud prediction in AMPS is a primary concern of this work.

AMPS simulations used for 0000 UTC 1 December 2015 - 1200 UTC 19 January 2016 employ Polar WRF 3.3.1 as described by Wille et al. (2017). Afterward, the AMPS forecast system was upgraded to Polar WRF 3.7.1 (Table 1). The update has no impact on our analyses for the WAIS Divide where all of the observations concluded prior to the change. Grid 2 at 10 km resolution has 667 by 628 horizontal grid points. The boundary layer is represented with the Mellor-Yamada-Janjić planetary boundary layer scheme with nonsingular implementation of level-2.5 Mellor-Yamada closure for turbulence in the planetary boundary layer and free atmosphere (Janjć., 1994). Cumulus is parametrized with the Kain-Fritsch scheme. The surface physics are represented with the 4-layer Noah land surface model with polar modifications (Bromwich et al., 2009; Hines et al., 2015). Other physics options include the Goddard shortwave radiation scheme (Chou et al., 2001), and the Rapid Radiative Transfer Model for GCMs (RRTMG, Clough et al., 2005) longwave radiation scheme. The WRF single-moment 5-class scheme (WSM5C, Hong et al., 2004) is employed to represent the cloud microphysics.

Formatted: Font color: Auto

3.2 Polar WRF 3.9.1 simulations

Additional numerical simulations during the time of the AWARE field program are conducted with Polar WRF version 3.9.1 (Table 1). These are single-domain simulations with the same grid and topography as AMPS grid 2 (Fig. 1b). The 60 vertical layers are identical to the AMPS simulations. In addition to AMPS, ~~we lean upon our experience with polar simulations for~~prior simulations of Polar WRF guide the selection of physical parameterizations (e.g., Wilson et al., 2011, 2012; Bromwich et al., 2013b; Cassano et al., 2017; Hines and Bromwich, 2017). The Mellor–Yamada–Nakanishi–Niino (MYNN; Nakanishi and Niino, 2006) level-2.5 scheme is used for the atmospheric boundary layer and the corresponding atmospheric surface layer. We use RRTMG for longwave and shortwave radiation. Cloud liquid water, cloud ice, and snow impact the shortwave and longwave radiation, but rain water is not used in the radiation calculations. Cumulus is parameterized with the Kain-Fritch scheme (Kain, 2004). The polar-optimized Noah land surface model is also used. ~~Similar to AMPS simulations for grid 2, no nudging is applied for the Polar WRF 3.9.1 simulations.~~ The PWRF 3.9.1 simulations presented here input fractional sea ice concentrations from gridded fields at 12.5 km resolution processed by l'Institut Francais de Recherché Pour l'Exploitation de La Mer (ftp://ftp.ifremer.fr/ifremer/). The sea ice fraction for 1200 UTC 10 January 2016 is shown in Fig. 2b. Sea ice albedo is set at 0.80, same as the snow albedo.

Formatted: Font color: Text 1

Formatted: Font color: Auto

One simulation, referred to as WRF GFS, is conducted with initial and boundary conditions taken from the GFS final analysis. The AMPS forecasts use the GFS forecasts by the same model which are available at the time. Thus, AMPS and WRF GFS are conducted with the same forecast system, although the products used will not be identical. Additional observations are assimilated into the final analysis. Initial and boundary conditions of meteorological fields for the other Polar WRF 3.9.1 simulations are interpolated from ERA-Interim reanalysis (ERA-I; Dee et al., 2011) fields available every 6

Formatted: Font color: Auto

Formatted: Font color: Auto

Formatted: Font color: Auto

h on 61 sigma levels and the surface at T255 resolution. We have made this change to obtain the best available agreement with observed clouds and radiation. Bracegirdle and Marshall (2012) found that ERA-I best represented the atmospheric circulation near Antarctica among the reanalyses they evaluated. Bromwich et al. (2013b) found that the boundary layer temperature fields were better represented in WRF simulations driven by ERA-I. Nudging toward analysis fields or observations is not performed on grid 2 during the forecast segment of the AMPS forecasts, and no nudging is included for the Polar WRF 3.9.1 simulations. Besides the microphysics schemes that are of interest to us, some differences between AMPS and Polar WRF 3.9.1 simulations will occur due to the different base versions of WRF, the source for driving initial and boundary conditions, and the data assimilation used for AMPS initialization. Strict equality between AMPS and Polar WRF simulations is not required for the goals of this paper, as we are interested in testing the sensitivity to the microphysics parameterization.

Formatted: Font color: Auto

Formatted: Font color: Auto

As shown in Table 1, four different schemes are employed for the cloud microphysics ~~, as we wish~~ to see ~~which~~how the schemes ~~most accurately represents~~impact the atmospheric hydrology and cloud radiative ~~impac~~effect. Listowski and Lachlan-Cope (2017) previously tested five schemes with Polar WRF 3.5.1 for simulations over the central Antarctic Peninsula, however, we are interested in two newer ~~advanced~~ schemes that have become available in more recent versions of WRF. Furthermore, WAIS Divide is more southerly, colder, and the local atmosphere is likely to be more pristine than over the Antarctic Peninsula, where the oceanic influence is strong.

First, we consider WSM5C as it is the microphysics scheme used for AMPS. This widely used scheme is computationally efficient and considers cloud water, cloud ice, rain, and snow as hydrometer classes. Cloud water and cloud ice are suspended, while rain and snow gradually precipitate out with a fall speed. Supercooled water is allowed to exist, and falling snow gradually melts at temperatures above 0°C. Given that the AMPS simulations and the new Polar WRF 3.9.1 simulations are not conducted with identical model configurations, the simulation referred to as WSM5C (Table 1) is required for comparisons.

Three more recent~~advanced~~ schemes are also tested. Following Hines and Bromwich (2017), the two-moment Morrison scheme (e.g., Morrison et al., 2005, 2009) is used as it has been extensively tested in the Arctic and known for its ability to simulate supercooled liquid water (e.g., Morrison et al., 2008; Klein et al., 2009; Solomon et al., 2011; 2014; 2015). It was amongst the best performing schemes in Listowski and Lachlan-Cope's (2017) simulations. This two-moment bulk microphysics scheme predicts mixing ratios for cloud water, cloud ice, rain, snow and graupel and number concentrations for cloud ice, snow, rain and graupel. Particle size distributions are specified with gamma functions. IN are parameterized according to the Cooper curve, with greater ice crystal concentrations at lower temperatures (Cooper, 1986). The prediction of two-moments (number concentration and condensate mixing ratio) allows a more robust treatment of the particle size distributions that are important for the microphysical process rates and cloud/precipitation evolution. The liquid water droplet concentration for clouds, however, is specified in the WRF implementation. The standard setting with WRF is 250 cm^{-3}. Hines and Bromwich (2017) found best results during the pristine ASCOS study in the ~~eastern~~ Atlantic sector of the Arctic when the value was reduced to 20 cm^{-3} or less. For our AWARE simulations, we have selected 50 cm^{-3}. The observations of Lachlan-Cope et al. (2016) and O'Shea et al. (2017) suggest liquid droplet concentrations are typically above 100 cm^{-3} for clouds over the Antarctic Peninsula and the Weddell Sea, respectively.

Simulations are also performed with the aerosol-aware Thompson microphysics (Thompson and Eidhammer, 2014) that is an advance~~ement~~ over the earlier Thompson et al. (2008) bulk microphysics scheme that was one-moment for cloud water and two-moment for cloud ice. This microphysics scheme accounts for cloud nucleating aerosol particles and five water species: Cloud water, cloud ice, rain, snow and graupel. The scheme includes first order aerosol treatment with interactive IN and CCN ~~cloud condensation nuclei (CCN)~~ concentrations ~~that can vary in a storm or a cloud~~. Nucleation or complete evaporation of hydrometeors deplete or add to condensation nuclei. Thus, the cloud-CCN process is now more interactive on a local scale. Cloud water, cloud ice and rain are treated with two-moment predictions, but snow with only single moment (mixing ratio) predictions. We refer to this scheme as the Thompson scheme. All cloud ice with diameters exceeding 200 microns are converted to snow, which tends to reduce cloud ice mixing ratios and ice particle diameters in comparison to other schemes (Greg Thompson, personal communication, 2017). Rather than using constant global values for CCN and IN that may be inappropriate for the polar regions, climatological values for CCN and IN are taken from a global dataset with spatial and monthly variability. The dataset is from a seven-year simulation ~~Monthly global values for water-friendly and ice friendly aerosols are from a seven year simulation~~ of the Goddard Chemistry Aerosol Radiation and Transport (GOCART) model.

The final microphysics scheme is the Morrison-Milbrandt P3 scheme (Morrison and Milbrandt, 2015) hereafter called the P3 scheme. The use of the WRF 3.9.1 in our simulations is motivated by the addition of the very recent P3 scheme to the microphysics options. The new scheme avoids the previous arbitrary categorization of frozen hydrometers into cloud and precipitation, and thus allows for a continuum of particle properties. Fall speed is now applied across the continuum, rather than being limited to precipitation. There are four ice mixing ratio variables: total mass, rime mass, rime volume, and number, allowing for four degrees of freedom. Liquid hydrometers use a standard two-moment approach with cloud and rain categories. The constant liquid droplet number, 400 cm^{-3}, is larger than the standard value for the Morrison scheme.

Both the P3 scheme and the Thompson scheme were unavailable in Polar WRF 3.5.1 when Listowski and Lachlan-Cope (2017) ran simulations for the Antarctic Peninsula. They tested the WSM5C, the WRF double moment scheme, the Morrison scheme, the older Thompson scheme (Thompson et al., 2008), and the Milbrandt scheme (Milbrandt and Yau, 2005). The older Thompson scheme lacks the aerosol predictive ability of the newer Thompson scheme, and is single moment in cloud water. The latter three schemes simulated clouds in best agreement with observations (Listowski and Lachlan-Cope 2017).

Formatted: Font color: Auto

Formatted: Font color: Auto

Formatted: Font color: Auto

Formatted: Font color: Auto

All schemes were unsuccessful in representing the supercooled water for some temperature ranges, but the results show that some schemes with more complicated ~~more advanced~~ microphysical parameterizations show improvements in representing Antarctic clouds.

Formatted: Font color: Auto

~~Initial and boundary conditions of meteorological fields for Polar WRF 3.9.1 simulations are interpolated from ERA-Interim reanalysis (ERA-I; Dee et al., 2011) fields available every 6 h on 61 sigma levels and the surface at T255 resolution. This differs from the GFS fields used for AMPS simulations. We have made this change to obtain the best available agreement with observed clouds and radiation. Bracegirdle and Marshall (2012) found that ERA-I best represented the atmospheric circulation near Antarctica among the reanalyses they evaluated. Bromwich et al. (2013b) found that the boundary layer temperature fields were better represented in WRF simulations driven by ERA-I. Nudging toward analysis fields or observations is not performed on grid 2 during the forecast segment of the AMPS simulations, and no nudging is included for the Polar WRF 3.9.1simulations. Besides the microphysics schemes that are of interest to us, some differences between AMPS and Polar WRF 3.9.1 simulations will occur due to the different base versions of WRF, the source for driving initial and boundary conditions, and the data assimilation used for AMPS initialization. Strict equality between AMPS and Polar WRF simulations is not required for the goals of this paper, as we are interested in testing the sensitivity to the microphysics parameterization.~~

The six~~five~~ simulations for this study are shown in Table 1. AMPS 3-hr output was retrieved for 1 December 2015 to 31 January 2016. Five~~our~~ Polar WRF 3.9.1 simulations~~ with different microphysics schemes~~ were then performed. AMPS has the same microphysics as the WSM5C and WRF GFS simulations. ~~, however~~Unlike the AMPS forecasts, we used 24 hourly points ~~, the length of run segments is longer with~~of the Polar WRF 3.9.1 run segments~~simulations~~. A ~~minimum of~~ 12-hour spin-up is taken for each segment initialized at 0000 UTC each day for 3 December 2015 to 19 January 2016. Output each hour for hours 12-35 is combined into fields spanning 1200 UTC 3 December 2015 to 1100 UTC January 2016. Polar WRF output is bilinearly interpolated from the four nearest grid points to the location of WAIS Divide.

4 Results

The time period of the December 2015-January 2016 field program at WAIS Divide includes a major melting event over the Ross Ice Shelf and the adjacent Siple Coast of West Antarctica (Nicolas et al., 2017). Temperature over the Ross Ice Shelf and West Antarctica increased after 10 January, and many observing sites there experienced maximum temperatures above freezing for several days during the melting event. Figure 2a shows meteorological fields near the onset of the melting event, including ~~The onset of the melting event is demonstrated by Fig 2a which shows~~ the sea level pressure field, 2 m temperature and 10 m wind speed from the WSM5C simulation at 1200 UTC 10 January. Nicolas et al. (2017) discuss the contribution of a blocking high between 90-120°W to the melting event. Correspondingly, Fig. 2a displays anticyclonic shear for the wind

Formatted: Font color: Auto

barbs at this location. Northerly winds produce widespread advection of warm air over the Ross and Amundsen Seas to the ice shelf and West Antarctica.

4.1 Temperature and radiation

Time series of the 2-m temperature at WAIS Divide for 7 - 15 January reveal large warming after 1200 UTC 10 January (Fig. 3a). The observed temperature increases by 13.6°C over 10 hours after the minimum, then increases further to -1.4°C at 1800 UTC 11 January. Warmer locations at lower elevations over West Antarctica ~~can be inferred to be above the freezing point and experiencing~~allow melting to occur (Nicolas et al., 2017). After a second peak of -1.8°C late on 12 January, the WAIS Divide temperature gradually cools. AMPS has a slight negative~~cold~~ bias prior to the warming, then a negative~~cold~~ bias of several degrees during the warm period that follows (Fig. 3a). Interestingly, the WSM5C simulation with Polar WRF 3.9.1 driven by ERA-I eliminates most of the negative~~cold~~ bias prior to 10 January and during the warm period. The minimum temperature, however, drops to -22.4°C at 0800 UTC on 10 January in WSM5C. The simulation known as WRF GFS is frequently warmer than AMPS for the time series shown in Fig. 3a, but is usually colder than WSM5C during this time.

Formatted: Font color: Auto

Table 2 shows statistics of simulations compared to observations. 1099 hourly observations are available for most meteorological variables from 0600 UTC on 4 December to 0000 UTC on 19 January. Only values every 3 hr are used for AMPS statistics, since output was available at these intervals, so means, biases and other statistics are impacted by the reduced number of values (367). For each variable, Table 2 shows observed averages, and the following rows show AMPS, WSM5C, Morrison, Thompson, and P3 statistics. The largest magnitude temperature bias is for AMPS, which has a negative ~~AMPS has a cold~~ bias of 1.6°C during the observed period, and this ~~is reflected~~appears in the time series shown in Fig. 3a. A negative~~cold~~ bias is still present in WSM5C. However, it is reduced to 0.3°C (Table 2). Both biases are statistically significant from zero at the 99% confidence level according to the Student's t-test. The bias for WRF GFS, -1.5°C, is similar to that of AMPS.

Formatted: Font color: Auto

Formatted: Font color: Auto

The reduced negative~~cold~~ bias for WSM5C can be understood following the sensitivity tests by Bromwich et al. (2013b) with driving by the GFS final analysis (FNL) and ERA-I. They found the sensitivity to the source for initial and boundary conditions varied depending upon season and the choice of physical parameterizations. Their comparison using Polar WRF 3.2.1 with the MYNN PBL and the RRTMG radiation scheme has the closest model configuration to that used for AMPS and the Polar WRF 3.9.1 simulations. They found that the 2 m temperature bias changed from -3.3°C to 0.1°C with the switch from driving by FNL to driving by ERA-I (see their Table 5). Furthermore, the 2 m dewpoint bias increased from 1.2°C to 4.0°C.

Figure 4 shows scatter plots of the 2 m temperature and downwelling longwave radiation. AMPS, WSM5C, and WRF GFS are shown in Fig. 4a. Morrison, Thompson and P3 have similar scatter fields for the 2 m temperature, so only Morrison is shown (Fig. 4b). The cold bias for AMPS is increased for temperature warmer than -8°C. Therefore, AMPS is unlikely to be able to properly represent West Antarctic melting events. Moreover, relatively warm events at WAIS Divide are likely to be associated with cloud cover. This is consistent with Fig. 4c, as the error in downwelling longwave radiation is larger when the incident is larger when the observed incident radiation at the surface is larger than 200 W m^{-2}. In contrast, the Morrison simulation shows the simulated temperature to cluster around the one to one line over the entire range of observed temperature (Fig. 4b). Also, Morrison, Thompson and P3 show less longwave error than AMPS, WSM5C, and WRF GFS when the observed downwelling radiation is greater than 270 W m^{-2} (Figs. 4c and 4d).

The warmer and moister atmosphere in the Polar WRF 3.9.1 simulations is demonstrated by vertical profiles of temperature and specific humidity biases compared to radiosonde observations (Fig. ~~4~~5). There is a general negative~~cold~~ bias, except near 1900 m above sea level where the positive biases reach up to ~~with the more advanced microphysics schemes near 1900 m above sea level where the biases reach~~ 0.8 to 0.9°C (Fig. 5~~4~~a). Thus, there is a weaker near-surface lapse in the simulations than the observations (not shown). The most extreme bias is the near-surface cold bias for AMPS that reaches 2.3°C. The cold bias for AMPS is also larger than 1°C between 3500 and 5100 m ASL.

An especially striking difference between the AMPS simulation forced with GFS and the simulations driven with ERA-I is shown in Fig. 5~~4~~b. AMPS is dryer than the radiosonde observations at WAIS Divide at all levels shown, especially in the lowest 3000 m ASL. The WSM5C simulation is slightly drier than the other Polar WRF simulations. The simulations with the newer~~advanced~~ microphysics schemes are moister than the observations just above the surface with biases as large as 0.13 g kg^{-1}. Above the boundary layer, the specific humidity biases are small, generally below as 0.03 g kg^{-1}, for the simulations with the ~~advanced~~newer microphysics. From Fig. 5~~4~~, we can attribute the differences between the AMPS and WSM5C simulations to the colder and drier atmosphere initiated with GFS initial conditions for AMPS.

Figures 3b and 6~~5~~b help to explain the near-surface temperature results. Downwelling longwave radiation shows a clear negative bias for both AMPS and WSM5C, but the magnitude is much larger for the former. Table 3, with contribution from SEBS observations for 7 December to 16 January, shows that the downwelling longwave bias is quite large, -41.5 W m^{-2} for AMPS. The bias is reduced to -14.8 W m^{-2} for WSM5C and -17.0 W m^{-2} for WRF GFS. The WRF GFS simulation also has a slightly larger downwelling shortwave radiation bias, 22.3 W m^{-2}, than the other Polar WRF 3.9.1 simulations. Since the WRF radiation biases for WRF GFS are not greatly different than those of the WSM5C simulation which has the same microphysics scheme, WRF GFS is not discussed further.

Formatted: Font color: Auto

Formatted: Font color: Auto

Formatted: Font color: Auto

Formatted: Font color: Auto

Formatted: Font color: Auto

The deficit in longwave radiation is ~~driving~~contributing to the negative~~cold~~ temperature bias. Even though the downwelling shortwave biases are positive for AMPS and WSM5C (Table 3), most of the solar flux is reflected by the ice~~as the~~ surface. Thus, the net radiation flux bias is negative, -3.3 W m^{-2} for AMPS. This is consistent with the greater impact of longwave cloud forcing than shortwave cloud forcing over Antarctica (Pavolonis and Key 2003). Since a negative bias in downwelling longwave radiation and a positive bias for downwelling shortwave radiation are found for both AMPS and WSM5C, we believe Polar WRF 3.9.1 simulations can be used to explore the cloud radiative biases that impact the~~in~~ AMPS forecasts, and to seek improvements. Downwelling and upwelling longwave biases for both AMPS and WSM5C are all statistically significant (Table 3).

Figure 6~~5~~ shows the diurnal cycles of average fields for 2-m temperature, downwelling longwave radiation, downwelling shortwave radiation, and upwelling shortwave radiation. The time periods for averaging are 4 December 2015 – 19 January 2016 for the temperature and 7 December 2015 – 16 January 2016 for the radiation terms. Simulated biases in these fields vary with time of day, with local noon near 1930 UTC. To provide an idea of the statistical significance of differences in Fig. 6~~5~~a, we use the Student's t-test for AMPS and the observations. The observed temperature time series was adjusted each hour of day by a constant value until the statistical significance of the model minus observed difference was at the boundary of the 95% confidence level. Accounting for autocorrelation in the temperature time series, the degrees of freedom was reduced by a factor of 3. Accordingly, the bias at which the statistical confidence would be 95% could be established. The error bars every 3 hrs in Fig. 6~~5~~a show the range next to the observations for which differences are not statistically significant. Since AMPS values and observations of the surface energy balance are simultaneously available only 4 times a day, we use the WSM5C simulation and the observations to determine the statistical significance error bars for Figs 6~~5~~b-d ~~and 5c~~ (every two hours beginning at 0100 UTC).

The AMPS mean temperature in the daily cycle is less than the observed value at all AMPS output times. Only 0300 UTC is not statistically significant. The observations have an earlier minimum of -16.0°C at 0700 UTC, while the AMPS minimum of -18.5°C occurs at 1200 UTC. The AMPS ~~cold~~negative bias, peaks at 1200 UTC (3.1°C). For the Polar WRF 3.9.1 runs, WSM5C is close enough to the observations to be within statistical uncertainty for most hours, except near the time of minimum temperature, when there is a negative~~cold~~ bias of~~of~~ 1-2°C. The simulations with more advanced microphysics schemes are warmer than the observations during the hours of decreasing temperature. P3 is warmest during these times with statistically significant biases of 1.1 to 1.7°C. The transition between run segments at 1200 UTC results in a temperature decrease of up to 2°C, but the change is much less for WSM5C. Starting at 1500 UTC, the Polar WRF 3.9.1 simulations show small temperature biases that are not statistically significant. At or just after the time of maximum temperature, the Polar WRF 3.9.1 simulations show ~~increased warm~~positive biases that are statistically significant for Morrison, Thompson and P3. Obviously, the choice of microphysics scheme ~~strongly~~ impacts the temperature bias at WAIS Divide by enough to

Formatted: Font color: Auto

Formatted: Font color: Auto

change the sign of the overall bias, and this is shown in Table 2 with positivewarm biases of 0.1, 0.5, and 0.7°C using the Morrison, Thompson, and P3 schemes, respectively.

For downwelling shortwave radiation (Fig. 65c), AMPS has statistically significant positive biases at all hours, with the bias peaking at 106 W m^{-2} at 1500 UTC. The bias is much reduced for the Polar WRF 3.9.1 simulations and not statistically significant at most observation times. The Morrison scheme, however, does show a statistically significant positive bias ahead of solar noon, while P3 shows a negative bias after solar noon. Fig. 6d shows P3 to be an outlier for upwelling shortwave radiation near the hours of maximum insolation. Table 3 shows that the overall biases for all times during the observing period are 70.4, 17.0, 19.8, 2.5, and -14.2 W m^{-2} for AMPS, WSM5C, Morrison, Thompson, and P3, respectively. All these biases are statistically significant at the 99% confidence level, except for the Thompson scheme for which the bias fails the 95% confidence test.

Formatted: Font color: Auto

Formatted: Font color: Auto

The shortwave results are encouraging and suggest that advanced changing the microphysics schemes can greatly alleviate, and perhaps even reverse Antarctic radiation biases in numerical simulations. It may appear odd, however, that the upwelling shortwave radiation shows negative biases for all the Polar WRF 3.9.1 simulations that do not coincide with downwelling biases. The difference can be explained by the specified snow albedo in the WRF Noah routine. The specified maximum snow albedo is 0.8 for Noah, and average simulation albedos are slightly below this value. The average observed albedo, however, is 0.843. Therefore, a higher fraction of solar insolation is reflected at WAIS Divide than in these simulations. This results in a deficit of upwelling shortwave radiation (Table 3, Fig. 65d). The deficit increases the net radiation and contributes to the positive temperaturewarm bias for the Morrison, Thompson and P3. The impact of the albedo can be seen in the slope of the temperature curves after 1200 UTC in Fig. 65a.

We ran a sensitivity test with segments initialized at 0000 UTC each day between 6 January and 16 January 2016. The active period for analysis is 1200 on UTC 6 January until 1100 UTC on 17 January. The settings were equal to the WSM5C, however, the albedo over glacial ice was increased to 0.84, closer to the observed albedo at WAIS Divide. For the used part of the segments (hours 12-35), the 2-m Temperature average was -12.4°C in the sensitivity test. That is, 1.6°C colder than WSM5C during the same period. That is almost twice the magnitude of the spread of the bias in Polar WRF 3.9.1 simulations shown in Table 2. We surmise that a more realistic surface albedo would likely result in a cold bias for the Polar WRF 3.9.1 simulations.

The observed downwelling longwave radiation (see Fig. 65b) has a mean value of 210.6 W m^{-2} (Table 3). AMPS shows a strong negative bias at all hours that peaks at -53.0 W m^{-2} at 1500 UTC. The magnitude of the bias is much reduced for WSM5C, but the deficit from the observations is statistically significant at the 95% confidence level except at 0300 UTC and 0500 UTC. The overall bias for all times is -14.8 W m^{-2} and is statistically significant at 99% confidence (Table 3). While there is a large difference between AMPS and WSM5C, the microphysics scheme is nevertheless associated with excess incoming shortwave radiation and a deficit in incoming longwave radiation. This is consistent with Listowski and Lachlan-Cope's (2017) WSM5C results over the Antarctic Peninsula. They also found that more advanced microphysics schemes (the Morrison scheme is the only advanced scheme used by both studies) can alleviate radiation errors. Similarly, the radiation results were improved here with the Morrison, Thompson and P3 schemes. While the WSM5C scheme lies outside the error bars at most hours, the other three schemes are within the error bars at most hours in Fig. 6b. Table 3 shows overall downwelling longwave biases of -7.9, 0.4, and 1.8 W m^{-2} for Morrison, Thompson and P3these schemes, respectively. The latter two biases are not statistically significant from zero. Correspondingly, Fig. 65b shows that the three advanced schemes do not have statistically significant biases at most hours. The Morrison scheme, however, does show deficits exceeding 14 W m^{-2} at 1300 and 1500 UTC. These longwave and shortwave results suggest strengths and weaknesses in the simulation of Antarctic clouds.

4.2 Clouds

Figure 76 shows the average diurnal cycle over 7 December – 17 January of longwave and shortwave cloud forcing at the surface for the simulations. Cloud forcing (CF) is defined following Eqn. (1):

$$CF = F_{\text{all sky}} - F_{\text{clear sky}}, \qquad (1)$$

where $F_{all\ sky}$ is the net all sky flux and $F_{clear\ sky}$ is the net clear sky flux that is estimated to occur without the presence of clouds. Cloud forcing represents the warming effect of clouds (or cooling in the case of negative values) and can be calculated for the longwave, shortwave, or combined flux. Pavolonis and Key (2003) used 1985-1993 data including Advanced Very-High-Resolution Radiometer on NOAA polar orbiting satellites and the International Satellite Cloud Climatology Project to estimate cloud forcing. They found summertime shortwave cloud forcing of about -10 to -18 W m^{-2} for the latitude of WAIS Divide. Longwave cloud forcing was 17-35 W m^{-2}. For more recent estimates, Scott et al. (2017) used the Clouds and the Earth's Radiant Energy System (CERES) CALIPSO-CloudSat-CERES-MODIS dataset (Kato et al., 2011) to obtain monthly surface cloud forcing. From 2007-2010 satellite observations for points near WAIS Divide, they found January values of 57.3, -29.1, and 28.3 W m^{-2} for longwave, shortwave, and net cloud forcing, respectively.

Polar WRF 3.9.1 produced clear sky flux values for longwave and shortwave radiation, so cloud forcing could be readily calculated. Clear sky shortwave fluxes were not available from AMPS.

Figure 76a clearly shows that the longwave cloud forcing for AMPS is weak, while the longwave cloud forcing for WSM5C is less than that of the more advancedrecent schemes. The results for AMPS and WSM5C are consistent with the coldnegative temperature biases during these simulations. P3 produces the greatest overall longwave cloud forcing, but the

Formatted: Font color: Auto

Formatted: Font color: Auto

Formatted: Font color: Auto

Formatted: Font color: Auto

Formatted: Font color: Auto

Formatted: Font color: Auto

impact varies somewhat with time of day. Thompson produces nearly as much longwave cloud forcing as P3. The overall averages are 12.2, 31.9, 37.1, 44.8, and 46.1 W m^{-2} for AMPS, WSM5C, Morrison, Thompson and P3, respectively.,. The simulated cloud values can be compared to monthly surface cloud forcing estimated by Scott et al. (2017) from the Clouds and the Earth's Radiant Energy System (CERES) CALIPSO-CloudSat-CERES-MODIS dataset (Kato et al., 2011). Using 2007-2010 satellite observations for points near WAIS Divide, they found January values of 57.3, -29.1, and 28.3 W m^{-2} for longwave, shortwave, and net cloud forcing, respectively. The simulated cloud forcing tends to be much greater than the climatological values of Pavolonis and Key (2003), yet smaller than Scott et al.'s (2017) values. Given that clouds contributed to the major melting event during January 2016 (Nicolas et al., 2017), cloud forcing in excess of the climatological mean is possible for this month.

Fig. 76b shows shortwave cloud forcing which has a cooling effect on the surface. There are considerable differences between the more recent advanced microphysics schemes. The overall averages are -11.0, -10.1, -13.7, and -18.5 W m^{-2} for WSM5C, Morrison, Thompson and P3, respectively. P3 shows a strong diurnal cycle with a minimum magnitude (-13.5 W m^{-2}) at 0800 UTC and a maximum magnitude (-25.2 W m^{-2}) at 2300 UTC near the time of maximum insolation and temperature. In contrast, the Morrison scheme has a minimum magnitude when insolation is largeshows a small diurnal variation. MThe more recentadvanced microphysics schemes produce stronger cloud radiative properties than the WSM5C scheme. Of the three recentadvanced schemes, P3 shows the strongest cloud radiative impact, while Morrison shows the least.

The average diurnal cycles of sensible heat flux and the conductive heat flux into the ice at WAIS Divide are shown in Fig. 78. The conductive flux was not directly measured by Nicolas et al. (2017), however, the flux was estimated from the residual of other terms in the surface energy balance. The diurnal cycle of sensible heat flux was greatly amplified in the simulations compared to the observations (Fig 78a). The positive sensible heat fluxes into the atmosphere are especially large near the time of maximum temperature, with a maximum of 32.3 W m^{-2} at 1900 UTC for P3. The maximum is much smaller for AMPS (15.3 W m^{-2}), which is colder. The overall average observed value is small, 0.9 W m^{-2} (Table 3). Modelled overall averages vary from 1.8 W m^{-2} for AMPS to 11.4 W m^{-2} for P3.

The conductive flux into the ice is a critical term for mass balance of West Antarctica. Therefore, it is important for modelling studies to be able to well represent this quantity. Positive values are expected during December and January when insolation is large. The overall average for the residual estimate of Nicolas et al. (2017) is 7.5 W m^{-2} during the observational period (Table 3). AMPS, which has a negative temperaturecold bias, also has a differencebias of -3.2 W m^{-2} forcompared to the estimated conductive flux of Nicolas et al. (2017). The overall biases are positive for all the Polar WRF 3.9.1 simulations, with values of 2.2, 2.1, 2.8, and 5.1 W m^{-2} for WSM5C, Morrison, Thompson, and P3, respectively. The large values during the warmer part of the day are key to the positive biases (Fig. 87b).

While the previous analysis has concentrated on radiation fields and the surface energy balance, we now more directly examine the observed and simulated clouds. Figure 98 shows the LWP for 2 - 18 January 2016. The uncertainty of observed LWP is 10 g m^{-2} (Cadeddu et al., 2009). Modelled LWP includes both suspended liquid cloud droplets and falling rain. LWP values above 0 are observed at most times, but AMPS and WSM5C simulate non-zero values only during 11-12 January (Fig. 98a). The results demonstrate the known difficulty of the WSM5C microphysics to simulating liquid water for polar clouds (e.g., Listowski and Lachlan-Cope, 2017). The more advanced microphysics schemes simulate liquid water much more frequently than WSM5C, but do not well represent the instantaneous observed liquid water (Fig. 98b). Therefore, we suggest that the simulation of liquid water in polar clouds remains problematic (e.g., King et al., 2015; Hines and Bromwich, 2017; Listowski and Lachlan-Cope, 2017).

Table 4 shows the average condensate over 0000 UTC 2 January to 0000 UTC 18 January. The average observed LWP, 23 g m^{-2}, is larger than in any of the simulations. The largest simulated value is 15.5 g m^{-2} for P3, consistent with magnitude of cloud forcing for this simulation (Fig. 76). Morrison has smaller LWP, 5.1 g m^{-2}, than Thompson or P3, corresponding to the weaker cloud forcing in Fig. 76. LWP is small, 0.43 g m^{-2}a and 0.88 g m^{-2}, respectively for AMPS and WSM5C, respectively. The radiative impact of microphysics schemes for WAIS appears to be strongly linked to the ability to simulate liquid water.

Caution should be applied in comparing the distributions of suspended and precipitation hydrometers between schemes since the definitions of such categories are arbitrary and poorly defined physically (Morrison and Milbrandt, 2015). The distribution of hydrometers can be helpful, however, in understanding the inner workings of a microphysics scheme and comparing the simulated amounts of liquid and ice. Simulated cloud water tends to be an order of magnitude or two larger than rain water. Little ice is simulated as graupel or rime. Morrison simulates an order of magnitude more snow than cloud ice, while the difference is two orders of magnitude for Thompson. In contrast, the simulations with the WSM5C microphysics produced high amounts of cloud ice but little amounts of snow. The total ice condensate in the WSM5C simulation, 21 g m^{-2}, is more than twice the value for AMPS, 10 g m^{-2}. More cloud ice in WSM5C can explain the greater cloud radiative impact compared to AMPS given that liquid water is rarely present (Figs. 76a and 98a). For the more advanced microphysics schemes, ice water path (IWP) varies from 15 g m^{-2} for Morrison to 23 g m^{-2} for Thompson and P3. Fig 87c indicates that the time series of IWP often show a rough similarity between schemes. Accordingly, the amount of liquid water appears to be a stronger factor in the difference between simulations results.

Figure 109 shows times series of cloud occurrence fraction at the WAIS Divide during the MWR availability period. Figure 109a shows values determined from the MPL observations. For the model, however, cloud fraction requires a definition. One

Formatted: Font color: Auto

earlier method was widely used and defined clouds diagnostically. Clouds fraction was determined based upon factors such as relative humidity, statistic stability and vertical velocity (Slingo, 1987). With prognostic cloud schemes, cloud fraction is not necessarily a simple function of the condensate, so we must consider what value is used for comparison with observations. One formula that has been used for comparison between model and observations is the . For the simulations, we use the model cloud fraction formulation of Fogt and Bromwich (2008) calibrated to manual McMurdo cloud fraction observations:

$$Cloud\ Fraction = 0.075\,LWP + 0.170\,IWP\ , \tag{2}$$

where the total cloud fraction, $Cloud\ Fraction$ is based upon the LWP and IWP in g m^{-2}. The cloud fraction is limited to the maximum value of 1. Cloud occurrence fraction from the MPL is not identical to standard observer-based cloud fraction observations (e.g., Wagner and Kleiss, 2016). However, the instantaneous model cloud fraction by Eq. (2) is typically one or very close to zero, so the effective differences between cloud fraction and cloud fraction occurrence is minimized for comparisons between model and observations. Eq. (2) is especially useful for time-average cloud fraction, although the liquid and ice water paths must be instantaneous values, not time-average values.

Formatted: Font color: Auto

The observed cloud occurrence fraction is frequently 1, and the average is 0.77 during this time (Fig. 810a). Cloud free times are more common for AMPS, thus the average is 0.32 (Fig. 108b). The Polar WRF 3.9.1 simulations show some similarity in their time series of cloud fraction, with average varying from 0.59 for WSM6C to 0.71 for P3. Microphysics schemes with stronger cloud radiative forcing have larger average total cloud fraction (Figs. 67 and 109).

Liquid cloud occurrence fraction is shown in Fig. 110. Only the first term on the right-hand side of Eq. (2) is used to define modelled liquid cloud fraction. Liquid clouds are frequently observed but are rarely simulated by AMPS (Fig. 110a). The Morrison scheme simulates liquid clouds much more frequently than WSM5C, but not as frequently as the observations. The Thompson and P3 schemes simulate liquid clouds more frequently than the Morrison scheme. Average liquid cloud fractions are 0.65, 0.01, 0.05, 0.20, 0.26 and 0.34 for the observations, AMPS. WSM5C, Morrison, Thompson, and P3, respectively.

Figure 121 shows the vertical distribution of cloud fraction. While the observed cloud fraction is again determined by surface-based MPL observations, Eq. (2) is inappropriate for point values of cloud fraction in a column. We select the mixing ratio 0.001 g kg^{-1} as the classic WRF minimum hydrometer threshold for cloud in the simulations. Model fraction is either 0 or 1 for total condensate concentrations below or above the threshold. The upper troposphere is not shown as the MPL attenuates through cloud layers.

Remote sensing at WAIS Divide detects clouds that are frequently present below 650 hPa (Fig. 121a). Detectable clouds decrease with height and are rarely observed above 500 hPa, but this is likely due to in part to attenuation of the lidar pulse at lower altitudes. Thus, it is not surprising thate simulated clouds are appear much deeper and frequently extend above 400 hPa (Fig. 121b-f). Furthermore, tThe minimum threshold of 0.001 g kg^{-1} allows model clouds with the density of very thin cirrus that may be difficult to observe. We found that simulated cloud tops (not shown) are sensitive to the specification of the threshold.

Figure 132 shows liquid cloud occurrence fraction to be more confined to the lower troposphere than total cloud occurrence fraction (Fig. 121). The simulated liquid clouds, when present, are near the surface for the simulations with the WSM5C microphysics (Figs. 132b and 132c). The more recentadvanced microphysics schemes simulate deeper liquid clouds than are observed by MPL.

Figure 143 shows the mean cloud fraction profiles above seaground level (ASGL) for 2 January to 16 January. As noted earlier, the MPL pulse attenuation likely results in some underestimation of both the total cloud and liquid occurrence fractions at higher elevations. Returning to Fig. 121 that shows shallow clouds with variable vertical structure observed by the MPL, while the simulations have deep, vertically aligned clouds, the means shown in Fig. 143 reflectdisplay this difference in vertical structure. The averaging of frequent deep cloud structures results in high mean values for the simulations, compared to the means of the more variable observations. Therefore, a vertically aligned cloud overlap better represents the simulated clouds than a random overlap. These stacked clouds reduce the modelled cloud fraction shown in Fig 109, as the middle cloud layer is on of top of the low cloud layer, rather than additive to the cloud fraction. The observed average total cloud fraction peaks at 0.51 at 1985 m ASGL (Fig 134a). The fraction decreases to 0.30 near 23500 m ASGL then 0.10 above 331500 m. The profiles suggest that there could be slightly elevated (liquid-bearing) cloud occurrence at 392135 m ASGL. The observed liquid cloud fraction is more surface-based with a peak of 0.28 at both 1915 and 1985 m ASGL, and decreasing values to 0.06 at 22410 m (Fig 134a).

The simulated cloud fraction profile peaks near the surface for AMPS and WSM5C (Fig. 143b). For AMPS (WSM5C), the maximum is 0.50 (0.64) at 8 m AGL (84 m) above the surface. Cloud fraction is higher for the recentadvanced microphysics schemes, with all having maxima above 0.64 at heights below 24600 m ASGL. Largest cloud fraction is 0.69 at 21365 m for Thompson. After decreasing with height up to 2000 m, simulated cloud fraction tends to stabilize with height above that. Differences between the simulated and observed cloud fraction profiles in Figs. 13b may be linked with the near-surface temperature bias shown in Fig. 4a.

The mean simulated liquid and ice cloud fractions are shown in Fig. 154. The values are from 2-16 January 2016, the same period used for the profiles in Fig. 54. Similar to the profile displayed in Fig. 13a, the observations show a more shallow

Formatted: Font color: Auto

peak in the lower troposphere than in the simulations. (Fig. 15a). The fractions are based upon the total liquid or ice content. P3 has a unique liquid profile that peaks at 0.26 at 23576 m ASGL. The Morrison and Thompson simulations have similar liquid cloud fraction profiles with double peaks between 21360 and 25700 m. The average profiles suggest frequent liquid cloud tops near 1000 m AGL. Liquid cloud fraction for WSM5C peaks at 0.05 at 464 m AGL. AMPS has a peak of just 0.017 in the lowest 50 m. The simulations with advanced microphysics schemes show a reflection of the observed secondary liquid peak above 2100 m AGL (Fig. 14a). Fig. 154b shows that ice is frequently present in the lowest 1000 m above the surface forof the simulations. All the simulations show maxima for ice in the lowest 500 m above the surface varying from 0.50 at 8 m for AMPS and 0.49 for P3 at 365 m to 0.64 for 85 m with WSM5C. The Polar WRF 3.9.1 simulations produce more ice cloud fraction than AMPS. It may be inferred from Fig. 14b that the higher clouds in the simulations are likely to be thin cirrus (ice) clouds.

Formatted: Font color: Auto

A sensitivity test referred to as P3-50, was based upon P3 to see if the setting of 400 cm^{-3} for the liquid droplet number concentration had an important impact on results of that simulation. We set the liquid concentration at 50 cm^{-3} in the sensitivity test, same as in the simulation with the Morrison microphysics. We use 1200 UTC 6 January – 1100 UTC 17 January 2016 as the active period for test results. P3-50 exhibited a reduction of the average LWP from 21 g m^{-2} to 16 g m^{-2}, compared to the parent simulation P3. The ice water path is less impacted and reduced by less than 7%. Figure 165 shows the 2-m temperature and surface downwelling shortwave and longwave radiation. The change in specified liquid concentration has small impact on the 2 m temperature, with the largest impact after 10 January when more noticeable amounts of liquid water were simulated (Figs. 98b and 165a). The average temperature in P3-50 (-9.6°C) is the same as in P3 over the test period. The downwelling shortwave radiation, however, is modified with the local noon on January 11, 14 and 15 showing insolation increases of 50-170 W m^{-2} (Fig. 165b). P3-50 is an improvement on these days. The impact on the downwelling longwave radiation is much smaller (Fig. 165c). Overall, P3-50 has a net increase (decrease) in 23.9 (2.6) W m^{-2} in downwelling shortwave (longwave) radiation compared to P3. Since most of the shortwave radiation is reflected off the Antarctic surface, the net impact on the near-surface temperature is small (Fig. 165a).

5 Summary and conclusions

The recent 2015-2017 AWARE field program provides a highly detailed set of remote sensing and surface observations that can be used to study the simulation Antarctic clouds and the surface energy budget. We focus on the December 2015 - January 2016 test period when observations were taken at WAIS Divide. These observations are used for comparison with the AMPS forecasting system and new simulations with Polar WRF 3.9.1. AMPS uses the WRF Single-Moment 5-Class microphysics, while the new Polar WRF 3.9.1 simulations are run with WSM5C and three more recentadvanced microphysics schemes. These are the Morrison 2-moment microphysics, the Thompson-Eidhammer aerosol-aware microphysics, and the new Morrison-Milbrandt P3 microphysics.coper

AMPS simulates few liquid hydrometers during austral summer at WAIS Divide, even though liquid clouds are frequently observed by the MPL, primarily a consequence of the WSM5C microphysics in AMPS. Consequently, downwelling shortwave radiation is excessive at the surface, while downwelling longwave radiation is too small. The WSM5C simulation with Polar WRF 3.9.1 has reduced biases of the same sign. The decreased magnitude in WSM5C appears due to GFS-forcing of initial and boundary conditions for AMPS and while ERA-I is used for WSM5C. Simulated hydrometers are overwhelmingly composed of ice with WSM5C.

The more advanced microphysics schemes show considerable improvement in the simulation of overall cloud fraction, liquid hydrometers, and cloud radiative effects. The instantaneous simulation of liquid remains somewhat problematic even given the improvements. The Morrison scheme simulates less LWC and weaker cloud radiative forcing than the Thompson and P3 schemes. P3 simulates the greatest LWC and cloud radiative effect. All schemes appear to underestimate total cloud fraction and liquid cloud fraction at the WAIS Divide. The vertical distribution of simulated cloud properties differs from observed profiles, with deeper clouds simulated than observed, although the MPL may not detect the upper regions of clouds due to attenuation.

In the near future,~~The work presented here may contribute to improvements to the AMPS simulations of clouds being sought by NCAR if computational efficiency can be achieved (Jordan Powers, personal communication 2018). Moreover,~~ the more extensive AWARE cloud observations at McMurdo over the full seasonal cycle will provide a basis for sensitivity tests designed to seek Antarctic optimizations to the advanced microphysics schemes used for the WAIS Divide. In particular, we plan to work with two more advanced implementations of the P3 microphysics (Milbrandt and Morrison, 2016). Sensitivity tests will also vary the background IN concentrations in simulations with the Thompson microphysics, as the limited observational evidence suggests that the contributing aerosol concentrations may vary or are unknown over a range of orders of magnitude.

Formatted: Font color: Auto

6 Code availability

The standard release of WRF can be downloaded from NCAR (https://www.mmm.ucar.edu/weather-research-and-forecasting-model). The polar optimizations can requested from http://polarmet.osu.edu/PWRF/registration.php.

7 Data availability

All the observations from the AWARE field campaign (including the reprocessed MPL data set) can be downloaded from the ARM Data Discovery website (http://www.archive.arm.gov/discovery/). AMPS forecast fields in original WRF format are available from http://www.earthsystemgrid.org/project/amps.html. Selected AMPS output fields for March 2006 - December 2016 for Grids 2-6 can be downloaded from http://polarmet.osu.edu/AMPS/.

8 Team list

Keith M. Hines

David H. Bromwich

Sheng-Hung Wang

Israel Silber

Johannes Verlinde

Dan Lubin

9 Author contribution

Keith Hines was the primary author and coordinated with the other authors. He conducted the Polar WRF simulations, downloaded and processed AWARE data, and processed the model data.

David Bromwich coordinated the Ohio State component of AWARE and was the primary co-author. He read and provided input on all drafts of the manuscript and helped plan the simulations.

Sheng-Hung Wang processed the AMPS data for the manuscript.

Isreal Silber processed the MPL and cloud mask data. He provided advice on the use of these data.

Johannes Verlinde coordinated the Penn State component of AWARE. He provided advice on Antarctic clouds and the AWARE data.

Dan Lubin was the overall coordinator of AWARE. He provided advice on Antarctic clouds and the AWARE project and helped to coordinate the use of CERES data.

10 Competing interests

The authors declare that they have no conflict of interest.

11 Disclaimer

Any opinions presented here are those of the manuscript authors alone and are not necessarily those of Atmospheric Chemistry and Physics.

12 Acknowledgments

This research is supported by DOE Grant DE-SC0017981 and NSF Grant PLR 1443443. Numerical simulations were performed on the Intel Xeon cluster at the Ohio Supercomputer Center, which is supported by the State of Ohio. We thank Julien Nicolas for providing rawinsonde, surface energy balance and LWP observations for WAIS Divide and Ryan Scott for providing cloud forcing derived from CERES. All the observations from the AWARE field campaign (including the

reprocessed MPL data set) can be downloaded from the ARM Data Discovery website (http://www.archive.arm.gov/discovery/). This is Contribution 1584~~XXXX~~ of the Byrd Polar & Climate Research Center.

13 References

Andreas, E.L, Horst, T.W., Grachev, A.A., Persson, P.O.G., Fairall, C.W., Guest, P.S., Jordan, R.E.: Parametrizing turbulent exchange over summer sea ice and the marginal ice zone, Q. J. Roy. Meteor. Soc., 136, 927-943, doi:10.1002/qj.618, 2010.

Barker, D.M., Huang, W., Guo, Y.-R., Bourgeois, A.J., Xiao, Q.-N.: A three-dimensional (3DVAR) data assimilation system for use with MM5: Implementation and initial results, Mon. Weather Rev., 132, 897-914, doi:10.1175/1520-0493(2004)132<0897:ATVDAS>2.0.CO;2, 2004.

Barlage, M., Chen, F., Tewari, M., Ikeda, K., Gochis, D., Dudhia, J., Rasmussen, R., Livneh, B., Ek, M., Mitchell, K.: Noah land model modifications to improve snowpack prediction in the Colorado Rocky Mountains, J. Geophys. Res., 115, D22101, doi:10.1029/2009JD013470, 2010.

Bracegirdle, T.J., Marshal, G.J.: The reliability of Antarctic tropospheric pressure and temperature in the latest global reanalyses, J. Climate, 25, 7138-7146, doi:10.1175/JCLI-D-11-00685.1, 2012.

Bromwich, D.H., Hines, K.M., Bai, L.S.: Development and testing of Polar WRF: 2. Arctic Ocean, J. Geophys. Res., 114, D08122, doi:10.1029/2008JD010300, 2009.

Bromwich, D.H., Nicolas, J.P., Hines, K.M., Kay, J.E., Key, E., Lazzara, M.A., Lubin, D., McFarquhar, G.M., Gorodetskaya, I., Grosvenor, D.P., Lachlan-Cope, T.A., van Lipzig, N.: Tropospheric clouds in Antarctica, Rev. Geophys., 50, RG1004, doi:10.1029/2011RG000363, 2012.

Bromwich, D.H., Nicolas, J.P., Monaghan, A.J., Lazzara, M.A., Keller, L.M., Weidner, G.A., and Wilson, A.B.: Central West Antarctica among the most rapidly warming regions on Earth, Nat. Geosci., 6, 139-145, doi:10:1038/NGEO1671, 2013a.

Bromwich, D.H., Otieno, F.O., Hines, K., Manning, K., Shilo, E.: Comprehensive evaluation of polar weather research and forecasting performance in the Antarctic, J. Geophys. Res., 118, 274-292, doi:10.1029/2012JD018139, 2013b.

Bromwich, D.H., Nicolas, J.P., Monaghan, A.J., Lazzara, M.A., Keller, L.M., Weidner, G.A., and Wilson, A.B.: Corrigendum: Central West Antarctica among the most rapidly warming regions on Earth, Nat. Geosci., 7, 76, doi:10.1038/ngeo2016, 2014.

~~Cadeddu, M.: ARM: Microwave Water Radiometer (MWR): Water Liquid and Vapor Along Line of Sight (LOS) Path (Atmospheric Radiation Measurement (ARM) Archive, Oak Ridge National Laboratory (ORNL), doi:10.5439/1046211, 1993.~~

Cadeddu, M.: G-Band Vapor Radiometer Profiler (GVRP) Handbook. DOE/SC-ARM/TR-16 091, Office of Science, DOE Office of Biological and Environmental Research, doi:10.2172/982364, 2010.

Cadeddu, M.P., Turner, D D., Liljegren, J.C.: A Neural Network for Real-Time Retrievals of PWV and LWP From Arctic Millimeter-Wave Ground-Based Observations, IEEE Transactions on Geoscience and Remote Sensing, 47, 1887–1900, doi:10.1109/TGRS.2009.2013205, 2009.

Cassano, J.J., DuViviera, A., Roberts, A., Hughes, M., Seefeldt, M., Brunke, M., Craig, A., Fisel, B., Gutowski, W., Hamman, J., Higgins, M., Maslowski, W., Nijssen, B., Osinski, R., Zeng, X.: Development of the Regional Arctic System Model (RASM): Near surface atmospheric climate sensitivity, J. Climate, 30, 5729-5753, doi:10.1175/JCLI-D-15-0775.1, 2017.

Chou, M.D., Suarez, M.J., Liang, X.Z., Yan, M.M.H.,: A thermal infrared radiation parameterization for atmospheric studies, NASA Tech. Memo, 104606, 56, doi:dopu.cs.auc.dk, 2001.

~~Clem, K.R., Fogt, R.L.: Varying roles of ENSO and SAM on the Antarctic Peninsula climate in austral spring, Geophys. Res., 118, 11481-11492, doi:10.1002/jgrd.50860, 2013.~~

Clough, S.A., Shephard, M.W., Mlawer, E.J., Delamere, J.S., Iacono, M.J., Cady-Pereira, K., Boukabara, S., Brown, P.D.: Atmospheric radiative transfer modeling: A summary of the AER codes, J. Quant. Spectrosc. Ra., 91, 233-244, doi:10.1016/j.jqsrt.2004.05.058, 2005.

Cook, D.: ARM: Surface Energy Balance System (SEBS) Handbook, Atmospheric Radiation Measurement (ARM) Archive, Oak Ridge National Laboratory, Argonne, IL, 2018.

Cooper, W.A.: Ice initiation in natural clouds, Precipitation Enhancement—A Scientific Challenge, Meteorol. Monogr., 29-32, 1986.

Deb, P., Orr, A., Hosking, J.S., Phillips, T., Turner, J., Bannister, D., Pope, J.O., Colwell, S.: An assessment of the Polar Weather Research and Forecasting (WRF) model representation of near-surface meteorological variables over West Antarctica, J. Geophys. Res., 121, 1532-1548, doi.org/10.1002/2015jd024037, 2016.

DeConto, R.M., Pollard, D.: Contributions of Antarctica to past and future sea level rise, Nature, 531, 591-597, doi:10.1038/nature17145, 2016.

Dee, D.P., Uppala, S.M., Simmons, A.J., Berrisford, P., Poli, P., Kobayashi, S., Andrae, U., Balmaseda, M.A., Balsamo, G., Bauer, P., Bechtold, P., Beljaars, A.C.M., van de Berg, L., Bidlot, J., Bormann, N., Delsol, C., Dragani, R., Fuentes, M., Geer, A.J., Haimberger, L., Healy, S.B., Hersbach, H., Holm, E.V., Isaksen, L.,i Kalberg, P., Kohler, M., Matricardi, M., McNally, A.P., Monge-Sanz, B.M., Morcrette, J.-J., Park, B.-K., Peubey, C., de Rosnay, P., Tavolato, C., Thepaut, J.-N., Vitart, F.: The ERA-Interim reanalysis: Configuration and performance of the data assimilation system, Q. J. Roy. Meteor. Soc., 137, 553-597, doi:10.1002/qj.828, 2011.

Dooraghi, M., Reda, I., Xie, Y., Morris, V., Andreas, A., Kutchenreiter, M., Habte, A., Sengupta, M.: ARM: Sky Radiation Sensor: 60-Second Downwelling Irradiances (Atmospheric Radiation Measurement (ARM) Archive, Oak Ridge National Laboratory (ORNL), doi:10.5439/1025281, 1996.

Formatted: Font color: Auto

Flynn, C.J., Mendoza, A., Zheng, Y., Mathurb, S.: Novel polarization-sensitive micropulse lidar measurement technique, Opt. Express, 15, 2785-2790. doi:10.1364/OE.15.002785, 2007.

Fogt, R.L., Bromwich, D.H.: Atmospheric moisture and cloud cover characteristics forecast by AMPS, Weather Forecast., 23, 914-930, doi:10.1175/2008/WAF2006100.1, 2008.

~~Fogt, R.L., Bromwich, D.H., Hines, K.M.: Understanding the SAM influence on the South Pacific ENSO teleconnection, Clim. Dynam., 36, 1555.1576, doi:10.1007/s00382-010-0905-0, 2011.~~

Grosvenor, D.P., Choularton, T.W., Lachlan-Cope, T., Gallagher, M., Crosier, J., Bower, K.N., Ladkin, R.S., Dorsey, J.R.: In-situ aircraft observations of ice concentrations within clouds over the Antarctic Peninsula and Larsen Ice Shelf, Atmos. Chem. Phys., 12, 11275-11294, doi:10.5194/acp-12-11275-2012, 2012.

Hines, K.M., Bromwich, D.H.: Development and testing of Polar Weather Research and Forecasting (WRF) model. Part I: Greenland Ice Sheet meteorology, Mon. Weather Rev., 136, 1971-1989, doi:10.1175/2007MWR2112.1, 2008.

Hines, K.M., Bromwich, D.H.: Simulation of late summer Arctic clouds during ASCOS with Polar WRF, Mon. Weather Rev., 145, 521-541, doi:10.1175/MWR-D-16-0079.1, 2017.

Hines, K.M., Bromwich, D.H., Bai, L.-S., Barlage, M., Slater, A.S.: Development and testing of polar Weather Research and Forecasting Model: Part III. Arctic land, J. Climate, 24, 26-48, doi:10.1175/2010JCLI3460.1, 2011.

Hines, K.M., Bromwich, D.H., Bai, L., Bitz, C.M., Powers, J.G., Manning, K.W.: Sea ice enhancements to Polar WRF, Mon. Weather Rev., 143, 2363.2385, doi:10.1175/MWR-D-14-00344.1, 2015.

Hogan, A.W.: Aerosol exchange in the remote troposphere, Tellus, 38, 197-213, 1986.

Holdridge, D., Kyrouac, J.: ARM: ARM-Standard Meteorological Instrumentation at Surface (Atmospheric Radiation Measurement (ARM) Archive, Oak Ridge National Laboratory (ORNL), doi:10.5439/1025220, 1993.

Hong, S.-Y., Dudhia, J., Chen, S.-H.: A revised approach to ice microphysical processes for the bulk parameterization of clouds and precipitation, Mon. Weather Rev., 132, 103-120, doi:10.1175/1520-0493(2004)132<0103:ARATIM>2.0.CO;2, 2004.

~~Hosking, J.S., Orr, A., Bracegirdle, T.J., Turner, J.: Future circulation changes off West Antarctica: Sensitivity of the Amundsen Sea Low to projected anthropogenic forcing, Geophys. Res. Lett., 43, 367-376, doi:10.1002/2015SGL067143, 2016.~~

Janjć, Z.I.: The step-mountain Eta coordinate model: Further developments of the convection, viscous sublayer, and turbulence closure schemes, Mon. Weather Rev., 122, 927-945, doi:10.1175/1520-0493(1994)122<0927:TSMECM>2.0.CO;2, 1994.

Kain, J.S.: The Kain - Fritsch convective parameterization: An update, J. Appl. Meteorol., 43, 170-181, doi:10.1175/1520-0450(2004)04360;0170:tkcpau62;2.0.co;2, 2004.

Kato, S., Rose F.G., Sun-Mack S., Miller W.F., Chen Y., Rutan D.A., Stephens G.L., Loeb N.G., Minnis P., Wielicki B.A., Winker D.M., Charlock T.P., Stackhouse P.W., Xu K.-M., Collins W.: Computation of top-of-atmosphere and surface irradiances with CALIPSO, CloudSat, and MODIS-derived cloud and aerosol properties. J. Geophys. Res., 116, D19209. doi:10.1029/2011JD016050, 2011.

King J.C., Gadian, A., Kirchgaessner, A., Kuipers, Munneke, P., Lachlan-Cope, T.A., Orr, A., Reijmer, C., van den Broeke, M.R., van Wessem, J.M., Weeks, M.: Validation of the summertime surface energy budget of Larsen C Ice Shelf (Antarctica) as represented in three high-resolution atmospheric models, J. Geophys. Res., 120, 1335-1347, doi:10.1002/2014JD022604, 2015.

Klein, S.A., McCoy, R.B., Morrison, H., Ackerman, A.S., Avramov, A., de Boer, G. Chen, M., Cole, J.N.S., Del Genio, A., Falk, M., Foster, M.J., Fridlind, A.M., Golaz, J.-C., Hashino, T., Harrington, J.Y., Hoose, C., Khairoutdinov, M., Larson, V.E., Liu, X., Luo, Y., McFarquhar, G., Menon, S., Neggers, R.A.J., Park, S., Poellot, M., Schmidt, J.M., Sednev, I., Shipway, B.J., Shupe, M.D., Spangenberg, D., Sud, Y.C., Turner, D.D., Veron, D.E., von Salzen, K., Walker, G., Wang, Z., Wolf, A.B., Xie, S., Xu, K., Yang, F., Zhang G.: Intercomparison of model simulations of mixed-phase clouds observed during the ARM Mixed-Phase Arctic Cloud Experiment. Part I: Single-layer cloud, Q. J. Roy. Meteor. Soc., 135, 979-1002, doi:10.1002/qj.416, 2009.

Lachlan-Cope, T., Listowski, C., O'Shea, S.: The microphysics of clouds over the Antarctic Peninsula. Part 1: Observations, Atmos. Chem. Phys., 16, 15605-15617, doi.org/10.5194/acp-16-15605-2016, 2016.

Lazzara, M.A., Weidner, G.A., Keller, L.M., Thom, J.E., Cassano, J.J.: Antarctic Automatic Weather Station Program: 30 years of polar observations, B. Am. Meteorol. Soc., 93, 1519-1537, doi:10.1175/BAMS-D-11-00015.1, 2012.

Listowski, C., Lachlan-Cope, T.: The microphysics of clouds over the Antarctic Peninsula. Part 2: Modelling aspects within Polar WRF, Atmos. Chem. Phys., 17, 10195-10221, doi:10.5194/acp-17-10195-2017, 2017.

Lubin, D., Chen, B., Bromwich, D.H., Somerville, R.C.J., Lee, W.-H., Hines, K.M.: The impact of Antarctic cloud radiative properties on a GCM climate simulation, J. Climate, 11, 447-462, doi:10.1175/1520-0442(1998)0112.0, 1998.

Mather, J.H., Voyles, J.W.: The ARM climate research facility: A review of structure and capabilities, B. Am. Meteorol. Soc., 94, 377.392, doi:0.1175/BAMS-D-11-00218.1, 2013.

McCoy, D.T., Hartmann, D.L., Zelinka, M.D., Ceppi, P., Grosvenor, D.P.: Mixed-phase cloud physics and Southern Ocean cloud feedback in climate models, J. Geophys. Res., 120, 9539-9554, doi:10.1002/2015JD023603, 2015.

Milbrandt, J.A., Morrison, H.: Parameterization of cloud microphysics based on the prediction of bulk ice particle properties. Part III: Introduction of multiple free categories, J. Atmos. Sci., 73, 975-995, doi.org/10.1175/JAS-D-15-0204.1, 2016.

Milbrandt, J.A., Yau, M.K.: A multimoment bulk microphysics parameterization. Part II: A proposed three-moment closure and scheme description, J. Atmos. Sci., 62, 3065-3081, doi.org/10.1175/JAS3535.1, 2005.

Morris, V.R.: Microwave radiometer (MWR) handbook. ARM-TR-016, DOE Office of Science, Office of Biological and Environmental Research, doi:10.2172/1020715, 2006.

Morrison, H., Milbrandt, J.A.: Parameterization of cloud microphysics based on the prediction of bulk ice particle properties. Part I: Scheme description and idealized tests, J. Atmos. Sci., 72, 287-311, doi.org/10.1175/JAS-D-14-0065.1, 2015.

Morrison, H., Pinto, J.O.: Intercomparison of bulk cloud microphysics schemes in mesoscale simulations of springtime Arctic mixed-phase stratiform clouds. Mon. Weather Rev., 134, 1880-1990, 2006.

Morrison, H., Curry, J.A., Khvorostyanov, V.I.: A new double-moment microphysics scheme for application in cloud and climate models. Part I: Description, J. Atmos. Sci., 62, 1665-1677, doi:10.1175/JAS3446.1, 2005.

Morrison, H., Pinto, J.O., Curry, J.A., McFarquhar, G.M.: Sensitivity of modeled Arctic mixed-phase stratocumulus to cloud condensation and ice nuclei over regionally varying surface conditions, J. Geophys. Res., 113, D05203, doi:10.1029/2007JD008729, 2008.

Morrison, H., Thompson, G., Tatarskii, V.: Impact of cloud microphysics on the development of trailing stratiform precipitation in a simulated squall line: Comparison of one- and two-moment schemes, Mon. Weather Rev., 137, 991-1007, doi:10.1175/2008MWR2556.1, 2009.

Nakanishi, M., Niino, H.: An improved Mellor-Yamada level-3 model: Its numerical stability and application to a regional prediction of advection fog, Bound.-Lay. Meteorol., 119, 397-407, doi:10.1007/s10546-005-9030-8, 2006.

Nicolas, J.P., Bromwich, D.H.: Climate of West Antarctica and influence of marine air intrusions, J. Climate, 24, 49-67, doi:10.1175/2010JCLI3322.1, 2011.

Nicolas, J.P., Bromwich, D.H.: New reconstruction of Antarctic near-surface temperatures: Multidecadal trends and reliability of global reanalyses, J. Climate, 27, 8070-8093, doi:10.1175/JCLI-D-13-00733.1, 2014.

Nicolas, J.P, Scott, R.C., Cadeddu, M.P., Bromwich, D.H., Verlinde, J., Lubin, D., Russell, L.M., Jenkinson, C., Powers, H.H., Ryczek, M., Stone, G., Wille, J.: January 2016 extensive summer melt in West Antarctica favoured by strong El Nino, Nat. Commun., 8, 15799, doi:10.1038/ncomms15799, 2017.

NOAA Environmental Modeling Center: The GFS Atmospheric Model. NCEP Office Note 442, 14 pp. [Available online at www.emc.ncep.noaa.gov /officenotes/newernotes/on442.pdf.], 2003.

O'Shea, S.J., Choularton, T.W., Flynn, M., Bower, K.N., Gallagher, M., Crosier, J., Williams, P., Crawford, I., Fleming, Z.L., Listowski, C., Kirchgaessner, A., Ladkin, R.S., Lachlan-Cope, T.: In situ measurements of cloud microphysics and aerosol over coastal Antarctica during the MAC campaign, Atmos. Chem. Phys., 17, 13049-13070, doi.org/10.5194/acp-17-13049-2017, 2017.

Pavolonis, M., Key, J.: Antarctic cloud radiative forcing at the surface estimated from the AVHRR Polar Pathfinder and ISCCP D1 datasets, 1985-93. J. Appl. Meteorol., 42, 827-840, doi:10.1175/1520-0450(2003)042<0827:ACRFAT>2.0.CO;2, 2003.

Powers, J.G., Manning, K.W., Bromwich, D.H., Cassano, J.J., Cayette, A.M.: A decade of Antarctic science support through AMPS, B. Am. Meteorol. Soc., 93, 1699-1712, doi:10.1175/BAMS-D-11-00186.1, 2012.

Pon, K.: The representation of low cloud in the Antarctic Mesoscale Prediction System, M.S. thesis, Atmospheric Sciences Program, Dept. of Geography, The Ohio State University, 80 pp, 2015.

Rignot, E.: Changes in West Antarctic ice stream dynamics observed with ALOS PALSAR data, Geophys. Res. Lett., 35, L12505, doi:10.1029/2008GL033365, 2008.

Formatted: Font color: Auto

Schmeisser, L., Backman, J., Ogren, J.A., Andrews, E., Asmi, E., Starkweather, S., Uttal, T., Fiebig, M., Sharma, S., Eleftheriadis, K., Vratolis, S., Bergin, M., Tunved, P., A. Jefferson, A.: Seasonality of aerosol optical properties in the Arctic, Atmos. Chem. Phys., 11,599–11,622, doi:10.5194/acp-18-11599-2018, 2018.

Scott, R.C., Lubin, D.: Unique manifestations of mixed-phase cloud microphysics over Ross Island and the Ross Ice Shelf, Antarctica, Geophys. Res. Lett., 43, 2936-2945, doi:10.1002/2013JD021132, 2016.

Scott, R.C., Lubin, D., Vogelmann, A.M., Kato, S.: West Antarctic Ice Sheet cloud cover and surface radiation budget from NASA A-Train satellites, J. Climate, 30, 6151-6170, doi:10.1175/JCLI-D-16-0644.1, 2017.

Screen, J.A., Simmonds, I.: Half-century air temperature change above Antarctica: Observed trend and spatial reconstructions, J. Geophys. Res., 117, doi:10.1029/2012JD017885.Shupe, M.D.: Clouds at Arctic atmospheric observatories. Part II: Thermodynamic phase characteristics. J. Appl. Meteorol. Clim., 50, 645–661, doi.org/10.1175/2010JAMC2468.1, 2011.

Shupe, M., Intrieri, J.: Cloud radiative forcing of the Arctic surface: The influence of cloud properties, surface albedo, and solar zenith angle, J. Climate, 17, 616-628, doi:10.1175/1520-0442(2004)017<0616:CRFOTA>2.0.CO;2, 2004.

Silber, I., Verlinde, J., Eloranta, E.W., Cadeddu, M.: Antarctic cloud macrophysical, thermodynamic phase, and atmospheric inversion coupling properties at McMurdo Station: I. Principal data processing and climatology, J. Geophys. Res., 123, 6099-6121, doi:10.1029/2018JD028279, 2018a.

Silber, I., Verlinde, J., Eloranta, E.W., Flynn, C.J., Flynn, D.M.: Reprocessed MPL data sets, doi:10.5439/1468777, 2018b.

Silber, I., Verlinde, J., Eloranta, E.W., Flynn, C.J., Flynn, D.M.: Polar liquid cloud base detection algorithms for high spectral resolution or micropulse lidar data, J. Geophys. Res., doi:10.1029/2017JD027840, 2018c.

Skamarock, W.C., Klemp, J.B., Dudhia, J., Gill, D.O., Barker, D.M., Duda, M.G., Huang, X.-Y., Wang, W., Powers, J.G: A description of the Advanced Research WRF Version 3, NCAR Tech, Note NCAR/TN-475+STR, 125 pp, 2008.

Slingo, J.M.: The development and verification of a cloud prediction scheme for the ECMWF model, Q. J. Roy. Meteor. Soc., 113, 899-927, doi:10.1002/qj.49711347710, 1987.

Solomon, A., Shupe, M.D., Persson, P.O.G., Morrison, H.: Moisture and dynamical interactions maintaining decoupled Arctic mixed-phase stratocumulus in the presence of a humidity inversion, Atmos. Chem. Phys., 11, 10,127-10,148, doi:10.5194/acp-11-10127-2011, 2011.

Solomon, A., Shupe, M.D., Persson, O., Morrison, H., Yamaguchi, T., Caldwell, P.M., de Boer, G.: The sensitivity of springtime Arctic mixed-phase stratocumulus clouds to surface-layer and cloud-top inversion-layer moisture sources, J. Atmos. Sci., 71, 574-595, doi:10.1175/JAS-D-13-0179, 2014.

Solomon, A., Feingold, G., Shupe, M.D.: The role of ice nuclei recycling in the maintenance of cloud ice in Arctic mixed-phase stratocumulus, Atmos. Chem. Phys., 15, 10,631.10,643, doi:10.5194/acp-15-10631-2015, 2015.

Steig, E.J. Schneider, D.P., Rutherford, S.D., Mann, M.E., Comiso, J.C., Shindell, D.T.: Warming of the Antarctic ice-sheet surface since the 1957 International Geophysical Year, Nature, 457, 459-462, doi:10.1038/nature07669, 2009.

Formatted: Font color: Auto

Thompson, G., T. Eidhammer, T.: A study of aerosol impacts on clouds and precipitation development in a large winter cyclone, J. Atmos. Sci., 71, 3636-3658, doi:10.1175/JAS-D-13-0305.1, 2014.

Thompson, G., Field, P.R., Rasmussen, R.M., Hall, W.D.: Explicit forecasts of winter precipitation using an improved bulk microphysics scheme. Part II: Implementation of a new snow parameterization, Mon. Weather Rev., 136, 5095-5115, doi:10.1175/2008MWR2387.1 2008.

Tjernström, M., Leck, C., Birch, C.E., Bottenheim, J.W., Brooks, B.J. Brooks, I.M., Bäcklin, L., Chang, R.Y.-W., de Leeuw, G., Di Liberto, L., de la Rosa11, S., Granath, E., Graus, M., Hansel, A., Heintzenberg, J., Held, A., Hind, A., Johnston, P., Knulst, J., Martin, M., Matrai, P.A., Mauritsen, T., Müller, M., Norris, S.J., Orellana, M.V., Orsini, D.A., Paatero, J., Persson, P.O.G., Gao, Q., Rauschenberg, C., Ristovski, Z., Sedlar, J., Shupe, M.D., Sierau, B., Sirevaag, A., Sjogren, S., Stetzer, O., Swietlicki, E., Szczodrak, M., Vaattovaara, P., Wahlberg, N., Westberg, M., Wheeler, C.R.: The Arctic Summer Cloud Ocean Study (ASCOS): overview and experimental design. Atmos. Chem. Phys., 14, 2823–2869, doi:10.5194/acp-14-2823-2014, 2014.

Turner, J., Lachlan-Cope, T.A., Colwell, S., Marshall, G.J., Connolley, W.M.: Significant warming of the Antarctic winter troposphere, Science, 311(5769), 1914.1917, doi.org/10.1126/science.1121652, 2006.

van Tricht K., Lhermitte, S., Lenaerts, J.T.M., Gorodetskaya, I.V., L'Ecuyer, T.S., Noah, B., van den Broeke, R., Turner D.D., van Lipzig, N.P.M.: Clouds enhance Greenland ice sheet meltwater runoff. Nat. Commun., 7, doi:10.1038/ncomms10266, 2016.

Wagenbach, D., Gorlach, U., Moser, K., Munnich, K.O.: Coastal Antarctic aerosol: the seasonal pattern of its chemical composition and radionuclide content, Tellus, 40B, 426-436, 1988.

Wagner, T.J., Kleiss, J.M.; Error characteristics of ceilometer-based observations of cloud amount, J. Atmos. Ocean. Tech., 33, 1557-1567, doi:10.1175/JTECH-D-15-0258.1, 2016.

Wille, J.D., Bromwich, D.H., Cassano, J.J., Nigro, M.A., Mateling, M.E., Lazzara, M.A.: Evaluation of the AMPS boundary layer simulations on the Ross Ice Shelf, Antarctica, with unmanned aircraft observations, J. Appl. Meteorol. Clim., 56, 2239-2258, doi:10.1175/JAMC-D-16-0339.1, 2017.

Wilson, A.B., Bromwich, D.H., Hines, K.M.: Evaluation of Polar WRF forecasts on the Arctic System Reanalysis domain: Surface and upper air analysis, J. Geophys. Res., 116, D11112, doi:10.1029/2010JD015013, 2011.

Wilson, A.B., Bromwich, D.H., Hines, K.M.: Evaluation of Polar WRF forecasts on the Arctic System Reanalysis domain. Part II. Atmospheric hydrologic cycle, J. Geophys. Res., 117, D04107, doi:10.1029/2011JD016765, 2012.

Witze, A.: Antarctic clouds studied for first time in five decades, Nature, 529, 12-12, doi:10.1038/529012a, 2016.

Formatted: Font color: Auto